
FAIRNESS WITHOUT HARM: AN INFLUENCE-GUIDED ACTIVE SAMPLING APPROACH

A PREPRINT

Jinlong Pang UC Santa Cruz jpang14@ucsc.edu	Jialu Wang UC Santa Cruz faldict@ucsc.edu	Zhaowei Zhu Docta.ai zzw@docta.ai	Yuanshun Yao ByteDance kevinyaowork@gmail.com
Chen Qian UC Santa Cruz cqian12@ucsc.edu	Yang Liu UC Santa Cruz yangliu@ucsc.edu		

ABSTRACT

The pursuit of fairness in machine learning (ML), ensuring that the models do not exhibit biases toward protected demographic groups, typically results in a compromise scenario. This compromise can be explained by a Pareto frontier where given certain resources (e.g., data), reducing the fairness violations often comes at the cost of lowering the model accuracy. In this work, we aim to train models that mitigate group fairness disparity without causing harm to model accuracy. Intuitively, acquiring more data is a natural and promising approach to achieve this goal by reaching a better Pareto frontier of the fairness-accuracy tradeoff. The current data acquisition methods, such as fair active learning approaches, typically require annotating sensitive attributes. However, these sensitive attribute annotations should be protected due to privacy and safety concerns. In this paper, we propose a tractable active data sampling algorithm that does not rely on training group annotations, instead only requiring group annotations on a small validation set. Specifically, the algorithm first scores each new example by its influence on fairness and accuracy evaluated on the validation dataset, and then selects a certain number of examples for training. We theoretically analyze how acquiring more data can improve fairness without causing harm, and validate the possibility of our sampling approach in the context of risk disparity. We also provide the upper bound of generalization error and risk disparity as well as the corresponding connections. Extensive experiments on real-world data demonstrate the effectiveness of our proposed algorithm.

1 Introduction

Machine Learning (ML) has dramatically impacted numerous optimization and decision-making processes across various domains, such as credit scoring [Siddiqi, 2005] and demand forecasting [Carboneau et al., 2008]. Algorithmic fairness embraces the principle, often enforced by law and regulations, that the decision-maker should not exhibit biases toward protected group membership [Zhu et al., 2023], identified by characteristics such as race, gender, or disability. However, the pursuit of fairness unavoidably results in a compromise scenario where reducing the fairness violations usually leads to a degradation in accuracy, which has been observed and verified by numerous literature [Menon and Williamson, 2018, Dutta et al., 2020, Zhao and Gordon, 2022, Wang et al., 2022a, Zhu et al., 2021]. Theoretically, the phenomenon can be understood through a Pareto frontier on the tradeoff between group fairness and accuracy [Wang et al., 2021a, Martinez et al., 2020, Balashankar et al., 2019, Wei and Niethammer, 2022]. That is, as illustrated in Figure 1, given certain resources such as training data, when a model has reached a point on the Pareto frontier, without more data resources, it is impossible that one can improve fairness without worsening off model accuracy.

One major source of unfairness and a major cause of the fairness-accuracy tradeoff is biased training data. If an unbiased and “fairer” dataset is available, we will be hopeful that unfairness can be alleviated without compromising accuracy. Furthermore, such a “fairer” dataset would allow for obtaining a fair and accurate model through the standard

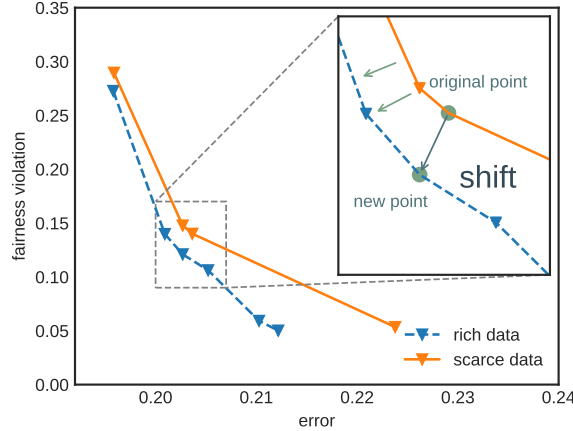


Figure 1: We compare the Pareto frontiers between the model trained with scarce data and that trained with rich data. Acquiring more data is capable of shifting the Pareto frontier toward lower disparity and lower error rates. In consequence, we can reach a new trade-off point that offers improved fairness and accuracy simultaneously, surpassing the original trade-off point.

empirical risk minimization (ERM) with cross-entropy (CE) loss. The above observation points to a promising way to improve fairness via actively acquiring more informative data, aiming to shift towards a better Pareto frontier of the fairness-accuracy trade-off [wik, Lipsey, 1975]. However, existing approaches that seek more data, such as fair active learning [Anahideh et al., 2022], typically require annotating sensitive attributes for training data. In practice, these sensitive attribute information such as race and gender, should be protected due to privacy regulations [Holstein et al., 2019, Andrus et al., 2021, Veale and Binns, 2017]. In the normal active learning scenario, collecting more data with sensitive attributes heightens privacy and safety risks due to the increased probability of leaking sensitive information.

Therefore, we ask the following question: *When not disclosing more annotations of training sensitive attributes, how can we acquire more data to improve model fairness without sacrificing accuracy?*

In this paper, we propose a tractable active data sampling algorithm in a *training sensitive attributes-free* way, which solely requires sensitive attributes on a *small validation set*. Particularly, the algorithm evaluates each example’s influence on fairness and accuracy using the validation dataset for ranking and then selects a certain number of examples to supplement the training set for training. We name our solution Fair Influential Sampling (FIS). The core challenge is approximating the corresponding influences of each new example without accessing its sensitive attributes. Technically, we evaluate the importance (influences) of each new example by comparing its gradient to that derived from the entire validation set. This comparison helps quantify the hypothesized change of group fairness disparity metric when adding this example to the training set. As a result, the requirement of training sensitive attributes can be relaxed, as gradient derivation serves as a role of fairness constraints to measure the group fairness disparity. The main contributions of our work are summarized as follows.

- We develop a tractable active data sampling algorithm (Algorithm 1) that does not rely on training sensitive attributes. The algorithm scores each new example based on the combined influences of prediction and fairness and then opts for a certain number of examples for training. [Section 4]
- We theoretically analyze how acquiring more data can improve fairness without harm from a distribution shift perspective view, and validate the possibility of our sampling approach in the context of risk disparity. We also provide the upper bound of generalization error and risk disparity as well as the corresponding connections (Theorem 5.1 and Theorem 5.2). [Section 5]
- Empirical experiments on real-world datasets (CelebA, Adult, and COMPAS) substantiate our claims, indicating the effectiveness and potential of our proposed algorithm in achieving fairness for ML classifiers. [Section 6]

2 Related Work

Fairness-accuracy tradeoff There are numerous work that have been successful at mitigating fairness disparities [Donini et al., 2018, Hardt et al., 2016, Agarwal et al., 2018, Zafar et al., 2017, Wang et al., 2022a]. However, these work typically rely on protected sensitive attributes of train examples to measure the fairness disparities across groups.

Moreover, it has been shown that there is a fairness-accuracy tradeoff, meaning that enforcing fair constraints heavily degrades the model performance. Notably, Chen et al. [Chen et al., 2022] characterized the change of the fairness violation when the data distribution is shifted. Except for training annotations, this paper does not work in the classical regime of the fairness-accuracy tradeoff. By properly collecting new data, we can improve both generalization and fairness, which cannot be achieved by working on a static training dataset that naturally incurs such a tradeoff. Besides, compared to prior works [Menon and Williamson, 2018, Prost et al., 2019], our method does not require additional assumptions about the classifier and the characteristics of the training/testing datasets (e.g., distribution shifts). Recent work [Li and Liu, 2022] utilizes the influence function to reweight the data examples but requires re-training. Our method focuses on soliciting additional samples from an external unlabeled dataset while [Li and Liu, 2022] reweights the existing and fixed training dataset.

Active learning The core idea of active learning is to rank unlabeled instances by developing specific measures, including uncertainty [Lewis and Catlett, 1994, Lindenbaum et al., 2004], representativeness [Dasgupta and Hsu, 2008], inconsistency [Wang et al., 2012], variance [Hoi et al., 2006], and error [Roy and McCallum, 2001]. A related line of work [Liu et al., 2021a, Wang et al., 2022b, Hammoudeh and Lowd, 2022, Xie et al., 2023] concentrates on ranking unlabeled instances based on the influence function. Compared to these studies with a focus on prediction performance, our work poses a distinct challenge taking into account fairness violations. Our approach is more closely with the *fair active learning* approach [Anahideh et al., 2022]. However, this framework still relies on training sensitive attributes and then unavoidably encounters the tradeoff between fairness and accuracy.

Fair classifiers without demographics Another line of work utilizes distributionally robust optimization (DRO) to reduce fairness disparity without relying on training sensitive attributes [Hashimoto et al., 2018, Kirichenko et al., 2022, Liu et al., 2021b, Lahoti et al., 2020, Veldanda et al., 2023, Sohoni et al., 2020]. Although these works evaluate the worst-case group performance in the context of fairness, their approaches differ as they do not strive to equalize the loss across groups. Besides, in these studies, accuracy and worst-case accuracy are used to showcase the efficacy of the proposed algorithms. Essentially, they equate fairness with uniform accuracy across groups, implying a model is considered fair if it demonstrates equal accuracies for all groups. However, this fairness definition is somewhat restrictive and inconsistent with common definitions such as DP or EOd.

Fair classification The fairness-aware learning algorithms, in general, can be categorized into pre-processing, in-processing, and post-processing methods. Pre-processing methods typically reweigh or distort the data examples to mitigate the identified biases [Asudeh et al., 2019, Azzalini et al., 2021, Tae and Whang, 2021, Sharma et al., 2020, Celis et al., 2020, Chawla et al., 2002, Zemel et al., 2013, Chen et al., 2018, Wang et al., 2021b]. More relevant to us is the *importance reweighting*, which assigns weights to training examples [Kamiran and Calders, 2012, Jiang and Nachum, 2020, Diesendruck et al., 2020, Choi et al., 2020, Qraitem et al., 2023, Li and Vasconcelos, 2019]. Our algorithm bears similarity to a specific case of importance reweighting, particularly the 0-1 reweighting applied to newly added data. Other parallel studies utilize importance weighting to learn a complex generative model in a weakly supervised setting [Diesendruck et al., 2020, Choi et al., 2020], or to mitigate representation bias in training datasets [Li and Vasconcelos, 2019]. Post-processing methods typically enforce fairness on a learned model through calibration [Feldman, 2015, Feldman et al., 2015, Hardt et al., 2016], but these work might not achieve the best fairness-accuracy tradeoff [Woodworth et al., 2017, Pleiss et al., 2017]. In contrast, these post-processing works still require sensitive attributes during the inference phase. Recent work Chen et al. [2023] develops a *bias score* classifier that operates independently of sensitive attributes; however, it is constrained to binary classifications.

3 Preliminaries

Problem setup We consider a standard K -class classification task whose training (test) data distribution is \mathcal{P} (\mathcal{Q}). Let $P := \{z_n\}_{n=1}^{|P|}$ represent the *training dataset* following distribution \mathcal{P} , where $|P|$ denotes the corresponding sample size. Each example, denoted as $z_n := (x_n, y_n)$, comprises two random variables: the *feature vector* x and the *label* y . The model trained on P is evaluated by the *test dataset* $Q := \{z_n^\circ\}_{n=1}^{|Q|}$, where $(\cdot)^\circ$ denotes that the data follows distribution \mathcal{Q} , each example $z_n^\circ := (x^\circ, y^\circ, s^\circ)$, and the sensitive group s_n° often refers to characteristics such as race, gender, etc. To align the fairness requirements on the test set Q with the model trained on P , a popular way is to exploit the sensitive attributes s [Donini et al., 2018, Wang et al., 2021a] or their proxies Zhu et al. [2023] in P and use them to formulate Lagrangians during training. However, extending these approaches to the active learning setting would require disclosing more sensitive attributes during sampling and training, which *contradicts* our goal. To avoid disclosing more sensitive attributes, we align the fairness requirements by a small hold-out *validation dataset* $Q_v := \{z_n^\circ\}_{n=1}^{|Q_v|}$ that is independent and identically distributed (IID) with the test set Q . We defer more technical details to Section 4.

Following the active learning setting, we would acquire new examples from a large *unlabeled dataset* $U := \{x'_n\}_{n=1}^{|U|}$ within a limited labeling budget $B(\ll |U|)$ [Liu et al., 2021a, Wang et al., 2022b, Hammoudeh and Lowd, 2022]. Denote the solicited example by $z'_n := (x'_n, y'_n)$, where y'_n is the ground-truth label. Note that the protected sensitive attributes from datasets P and U remain undisclosed during sampling and training. In this paper, we aim to incrementally update a model that was initially trained on P using standard ERM, by incorporating newly solicited data z'_n , such that the model can improve fairness without worsening model accuracy. Thus, the core challenge is efficiently determining new examples that induce a significantly better Pareto frontier. In the proceeding section 4, we shall delve into how to acquire new data.

Fairness definition We introduce the notions of fairness as follows.

Definition 3.1. (*Risk disparity* [Hashimoto et al., 2018, Zafar et al., 2019, Agarwal et al., 2019]). Define Q_k as the subset of Q corresponding to group k . Given the optimized model parameters \mathbf{w}^P trained on set P , risk disparity is defined as: $\mathcal{R}_{Q_k}(\mathbf{w}^P) - \mathcal{R}_Q(\mathbf{w}^P)$, where $\mathcal{R}_Q(\mathbf{w}) := \mathbb{E}_{z \sim Q}[\ell(\mathbf{w}, z)]$ denotes expected risk induced on target distribution Q .

Definition 3.1 naturally quantifies the discrepancy in a trained model's performance between a specific group set Q_k and the entire test set Q . That is, a model can be deemed fair if it exhibits consistent performance for a group set Q_k as compared to the test dataset Q . In settings such as face or speech recognition, this fairness definition implies the necessity for all demographic groups to receive the same quality service [Buolamwini and Gebru, 2018]. For completeness, we also include two well-known definitions of fairness:

Definition 3.2. (*Demographic Parity (DP)*). A classifier f adheres to demographic parity concerning the sensitive attribute s if: $\mathbb{E}[f(\mathbf{w}, x)] = \mathbb{E}[f(\mathbf{w}, x)|s]$.

Definition 3.3. (*Equalized Odds (EOd)* [Hardt et al., 2016]). A classifier f meets the equalized odds with respect to the sensitive attribute s if: $\mathbb{E}[f(\mathbf{w}, x)|y] = \mathbb{E}[f(\mathbf{w}, x)|y, s]$.

Even though there may be a general incompatibility between risk disparity and popular group fairness metrics like DP and EOd, under the criteria of the proposed fairness notion, these definitions could be encouraged [Shui et al., 2022, Hashimoto et al., 2018]. More details and proof can be found in the Appendix B.

Proposition 3.1. (*Informal*) Under appropriate conditions, the risk disparity can serve as a lower bound for fairness disparities based on common fairness definitions, such as DP and EOd.

Remark 3.1. (*Connections to other fairness definitions*) Definition 3.1 targets group-level risk fairness, which has similar granularity to other fairness notions such as accuracy parity [Zafar et al., 2017], device-level parity [Li et al., 2019], small accuracy loss for groups [Zafar et al., 2019, Balashankar et al., 2019, Martinez et al., 2019, Hashimoto et al., 2018], and bounded group loss [Agarwal et al., 2019].

4 Improving Fairness without Harm via Data Influential Sampling

In this section, we first introduce how to measure the importance (influence) of each example on accuracy and fairness without using the corresponding sensitive attributes, respectively. Then, we propose an influence-guided sampling algorithm that actively acquires new data based on the influences for further training.

4.1 Finding Influential Examples

To avoid using training sensitive attributes, our primary idea is to find newly acquired data that assists in creating a “fairer” dataset, which allows for training a fair and accurate model via standard ERM. Initially, we explore whether newly acquired data enhances fairness by examining the training process, where the model is typically updated using gradient descent. The change of model parameters by performing one step gradient descent on newly acquired data z' is

$$\mathbf{w}_{t+1} = \mathbf{w}_t - \eta \cdot \partial_{\mathbf{w}_t} \ell(\mathbf{w}_t, z') \quad (1)$$

where η refers to the learning rate and $\ell(\cdot)$ is the training loss function. It should be noted that before we solicit the true labels of samples z' , we first use proxy labels. In the following subsection 4.2, we will present a strategy for proxy labels. Training on z' affects the model's prediction on validation data z_n° regarding both accuracy and fairness. If the updated model \mathbf{w}_{t+1} outperforms the previous one \mathbf{w}_t evaluated on the validation dataset in terms of fairness and accuracy, this acquired data z' helps to reduce the fairness disparity without worsening accuracy.

To separately measure the accuracy and fairness performance of the updated model on the validation set, we introduce two types of loss functions: **fairness loss** $\phi(\mathbf{w}, z_n^\circ)$ and **accuracy loss** $\ell(\mathbf{w}, z_n^\circ)$, where validation data $z_n^\circ = (x_n^\circ, y_n^\circ, s_n^\circ)$. Note that these loss functions are developed for sampling, not for training. Besides, training loss function $\ell(\cdot)$ can be

reused as the accuracy loss function due to the same update target. One can identify training loss $\ell(\cdot, z')$ and accuracy loss $\ell(\cdot, z_n^\circ)$ based on the input data used. Without loss of generality, we assume that $\ell(\cdot)$ and $\phi(\cdot)$ are differentiable w.r.t. \mathbf{w} . Here, we do not restrict the generality of the fairness loss function; it can be any smoothed version of fairness metrics such as DP or EOD. Following this, we develop the influence of the accuracy and fairness components for finding the samples, respectively.

Influence of accuracy component When model parameters are updated from \mathbf{w}_t to \mathbf{w}_{t+1} by adding a new example z' , the influence of model's accuracy on one validation example z_n° is:

$$\text{Infl}_{\text{acc}}(z', z_n^\circ; \mathbf{w}_t, \mathbf{w}_{t+1}) := \ell(\mathbf{w}_{t+1}, z_n^\circ) - \ell(\mathbf{w}_t, z_n^\circ).$$

For ease of notation, we use $\text{Infl}_{\text{acc}}(z', z_n^\circ)$ to represent $\text{Infl}_{\text{acc}}(z', z_n^\circ; \mathbf{w}_t, \mathbf{w}_{t+1})$. By applying first-order Taylor expansion, we obtain the following closed-form statement:

Lemma 4.1. *The accuracy influence of new example z' on the validation dataset Q_v is:*

$$\text{Infl}_{\text{acc}}(z') := \sum_{n \in |Q_v|} \text{Infl}_{\text{acc}}(z', z_n^\circ) \approx -\eta \sum_{n \in |Q_v|} \langle \partial_{\mathbf{w}_t} \ell(\mathbf{w}_t, z'), \partial_{\mathbf{w}_t} \ell(\mathbf{w}_t, z_n^\circ) \rangle \quad (2)$$

Intuitively, the more negative $\text{Infl}_{\text{acc}}(z')$ is, the more positive the model accuracy (performance) that example z' can provide.

Influence of fairness component When model parameters are updated from \mathbf{w}_t to \mathbf{w}_{t+1} by adding a new example z' , the influence of model's fairness on one validation example z_n° is:

$$\text{Infl}_{\text{fair}}(z', z_n^\circ; \mathbf{w}_t, \mathbf{w}_{t+1}) := \phi(\mathbf{w}_{t+1}, z_n^\circ) - \phi(\mathbf{w}_t, z_n^\circ). \quad (3)$$

For simplicity, we write $\text{Infl}_{\text{fair}}(z', z_n^\circ; \mathbf{w}_t, \mathbf{w}_{t+1})$ as $\text{Infl}_{\text{fair}}(z', z_n^\circ)$. Then, similarly, we have:

Lemma 4.2. *The fairness influence of new example z' on the validation dataset Q_v is:*

$$\text{Infl}_{\text{fair}}(z') := \sum_{n \in |Q_v|} \text{Infl}_{\text{fair}}(z', z_n^\circ) \approx -\eta \sum_{n \in |Q_v|} \langle \partial_{\mathbf{w}_t} \ell(\mathbf{w}_t, z'), \partial_{\mathbf{w}_t} \phi(\mathbf{w}_t, z_n^\circ) \rangle \quad (4)$$

Similar to the accuracy component, the greater the negativity of $\text{Infl}_{\text{fair}}(z')$ is, the greater the positive impact that the example z' has on fairness.

Intuitions These two components evaluate the accuracy and fairness impact of each example by comparing the gradient originating from a single data sample with the gradient derived from the entire validation set, respectively. This comparison helps quantify the potential advantage of including this specific example in training. For instance, if the gradient obtained from one example has a similar direction to the gradient from the validation set, it indicates that incorporating this example contributes to enhancing the model's fairness or accuracy.

Training sensitive attributes are not disclosed One can easily check that neither the influence of accuracy nor fairness components require the sensitive attributes of any example z' , as the example z' only appears in the first-order gradient of the train loss $\partial_{\mathbf{w}_t} \ell(\mathbf{w}_t, z')$. In the fairness component, calculating the $\partial_{\mathbf{w}_t} \phi(\mathbf{w}_t, z_n^\circ)$ only relies on validation example z_n° 's sensitive attributes. Here, we also validate how accurate the first-order estimation of the influence is in comparison to the real influence [Koh and Liang, 2017], and find that the estimated influences for most of the examples are very close to their actual influence values. We refer the readers to Appendix C.1 for more details.

4.2 Algorithm: Fair Influential Sampling (FIS)

Following Lemma 4.1 and Lemma 4.2, we can efficiently select those examples with the most negative fairness influence and negative accuracy influence. This sampling method aids in reducing fairness disparities without worsening model accuracy.

Labeling Before presenting our sampling algorithm, it is necessary to address the problem of not accessing the true labels of new solicited examples. Lacking the label information for new examples poses a challenge in determining the corresponding influence on accuracy and fairness, a fact that is substantiated by Lemma 4.1 and Lemma 4.2. Intuitively, one can always recruit human annotators to get the ground-truth labels for those unlabeled examples. However, it is impractical due to the limited labeling budgets. To tackle this problem, another common approach is utilizing a model that has been effectively trained on dataset P to produce proxy labels, which serve to approximate the calculation of influences for examples from a substantial unlabeled dataset U . It's important to note that these proxy labels are

exclusively used during the sampling phase. To maintain good model performance, we still need to inquire about the true labels of the selected data examples for subsequent training. Here, we propose to annotate the proxy labels with the model trained on the labeled set P . In particular, we introduce a strategy that employs lowest-influence labels for annotating label \hat{y}' given x' :

$$\hat{y}' = \arg \min_{k \in \{1, \dots, K\}} |\text{Infl}_{\text{acc}}(x', k)|, \quad (5)$$

which corresponds to annotating the most confident label class. Denote by $\hat{z}' := (x', \hat{y}')$.

Algorithm 1 Fair influential sampling (FIS)

- 1: **Input:** training set P , unlabeled set U , validation set Q_v , new acquired set $S_t = \{\}$, $\forall t \in [T]$ rounds, number of new selected examples in each round r .
- 2: **Warmup:** Train a classifier f solely on P by minimizing the empirical risk R_ℓ . Obtain model parameters \mathbf{w}_1 and validation accuracy (on Q_v) VAL_0 .
- 3: **for** t in $\{1, 2, \dots, T\}$ **do**
- 4: Guess proxy label \hat{y}' for new examples \hat{z}' using Eq. (5).
- 5: Compute the influence of accuracy and fairness component using Eq. (2) and Eq. (4):
- 6: $S_{\text{original}} = \{\text{Infl}_{\text{fair}}(\hat{z}') \mid \text{Infl}_{\text{acc}}(\hat{z}') \leq 0, \text{Infl}_{\text{fair}}(\hat{z}') \leq 0, \hat{z}' \in U\}$
- 7: **while** $|S_t| < r$ **do**
- 8: Find top- $(r - |S_t|)$ annotated examples \hat{z}'_n based on the lowest fairness influence and then inquire about true labels y' :
- 9: $\{z'_n\} \xleftarrow{\text{inquiring}} \{\hat{z}'_n\} \leftarrow \text{Top-}(r - |S_t|)(S_{\text{original}})$
- 10: $S_t \leftarrow S_t \cup \{z'_n \mid \text{Infl}_{\text{acc}}(z'_n) \leq 0, \text{Infl}_{\text{fair}}(z'_n) \leq 0\}$
- 11: $U \leftarrow U \cap S_t; S_{\text{original}} \leftarrow S_{\text{original}} \cap S_t$
- 12: **end while**
- 13: Continue to train the model f on the set S_t via standard ERM. Obtain the updated model parameters \mathbf{w}_{t+1} . If the model's validation accuracy (on Q_v) VAL_t does not meet the desired threshold VAL_0 , reject the updated model.
- 14: **end for**
- 15: **Output:** models $\{\mathbf{w}_t \mid \text{VAL}_t > \text{VAL}_0\}$

Proposed algorithm The full procedure is outlined in Algorithm 1. Note that the tolerance ϵ is applied to monitor the performance drop in validation accuracy. In Line 2, we initiate the process by training a classifier f solely on dataset P , that is, performing a warm start. Subsequently, T -round sampling iterations are applied to acquire more examples to dataset P . Following the iterative fashion, FIS guesses labels using Eq. (5) in Line 4. Then, we calculate the scores for proxy examples based on the accuracy and fairness influence using Eq. (2) and Eq. (4) respectively. In Lines 6-10, we would opt for r samples based on the influence scores, and inquire about the true labels of these examples. However, due to the gap between proxy labels \hat{y}' and true label y , the accuracy and fairness influences of the top- r samples based on inquired true labels z' may not necessarily satisfy the same conditions ($\text{Infl}_{\text{acc}}(z') \leq 0, \text{Infl}_{\text{fair}}(z') \leq 0$). Therefore, we use a while loop to iteratively select the top- $(r - |S_t|)$ examples for labeling until we obtain r samples whose fairness influences based on true labels meet the conditions. Subsequently, in Line 9, we update sets U and S_{original} to prevent duplicate sampling. In Line 11, we would continue training using new examples with true inquired labels from set S_t . We save the model parameters at each round as checkpoints \mathbf{w}_t . To avoid potential accuracy drops incurred by excessively large random perturbations, we exclusively choose and offer models for output whose validation accuracy exceeds the initial validation accuracy VAL_0 . Although we propose a specific strategy for guessing labels, our algorithm is flexible and compatible with other labeling methods. A comparative analysis of computational costs is detailed in Appendix C.2.

5 How More Data Improves Fairness Without Harm?

In general, acquiring new data to supplement the original training dataset would potentially raise the distribution shift problem, affecting both accuracy and fairness. In this section, from a distribution shift perspective view, we first present a generalization error bound (accuracy side, Theorem 5.1) and risk disparity bound (fairness side, Theorem 5.2). The theoretical results jointly provide a high-level key insight that controlling the negative impact of distribution shift on generalization error, which refers to the model accuracy, could allow for improving fairness without harm. This theoretical insight validates the possibility of our sampling approach.

Without loss of generality, we discretize the whole distribution space and suppose that the train/test distributions are both drawn from a series of component distributions $\{\pi_1, \dots, \pi_I\}$ [Feldman, 2020]. Then, the empirical risk $\mathcal{R}_P(\mathbf{w})$

calculated over a training set P can be reformulated by splitting samples based on the component distributions:

$$\mathcal{R}_P(\mathbf{w}) := \mathbb{E}_{z \in P}[\ell(\mathbf{w}, z)] = \sum_{i=1}^I p^{(P)}(\pi = i) \cdot \mathbb{E}_{z \sim \pi_i}[\ell(\mathbf{w}, z)]. \quad (6)$$

where $p^{(P)}(\pi = i)$ represents the frequencies of examples in P drawn from component distribution π_i . Then, we can define the measure of probability distance between two sets or distributions as $\text{dist}(\mathcal{A}, \mathcal{B}) := \sum_{i=1}^I |p^{(\mathcal{A})}(\pi = i) - p^{(\mathcal{B})}(\pi = i)|$. To reflect the implicit unfairness in the models, we introduce two basic assumptions in convergence analysis [Li et al., 2019].

Assumption 5.1. (*L-Lipschitz Continuous*). *There exists a constant $L > 0$, for any $\mathbf{v}, \mathbf{w} \in \mathbb{R}^d$, $\mathcal{R}_P(\mathbf{v}) \leq \mathcal{R}_P(\mathbf{w}) + \langle \nabla \mathcal{R}_P(\mathbf{w}), \mathbf{v} - \mathbf{w} \rangle + \frac{L}{2} \|\mathbf{v} - \mathbf{w}\|_2^2$.*

Assumption 5.2. (*Bounded Gradient on Random Sample*). *The stochastic gradients on any sample z are uniformly bounded, i.e., $\mathbb{E}[\|\nabla \mathcal{R}_P(\mathbf{w}_t, z)\|^2] \leq G^2$, and training epoch $t \in [1, \dots, T]$.*

Analogous to Assumption 5.2, we further make a mild assumption to bound the loss over the component distributions π_i according to the corresponding model, that is, $\mathbb{E}_{z \sim \pi_i}[\ell(\mathbf{w}^P, z)] \leq G_P, \forall i \in I$. For completeness, we first analyze the upper bound of generalization error, specifically from the standpoint of distribution shifts.

Theorem 5.1. (*Generalization error bound*). *Let $\text{dist}(\mathcal{P}, \mathcal{Q})$, G_P be defined therein. With probability at least $1 - \delta$ with $\delta \in (0, 1)$, the generalization error bound of the model trained on dataset P is*

$$\mathcal{R}_Q(\mathbf{w}^P) \leq \underbrace{G_P \cdot \text{dist}(\mathcal{P}, \mathcal{Q})}_{\text{distribution shift}} + \sqrt{\frac{\log(4/\delta)}{2|P|}} + \mathcal{R}_P(\mathbf{w}^P). \quad (7)$$

Note that the generalization error bound is predominantly impacted by the shift in distribution, especially when we consider an overfitting model, i.e., the empirical risk $\mathcal{R}_P(\mathbf{w}^P) \rightarrow 0$.

Theorem 5.2. (*Upper bound of risk disparity*). *Suppose $\mathcal{R}_Q(\cdot)$ follows Assumption 5.1. Let $\text{dist}(\mathcal{P}, \mathcal{Q})$, G_P , $\text{dist}(\mathcal{P}_k, \mathcal{Q}_k)$ and $\text{dist}(\mathcal{P}_k, P)$ be defined therein. Given model \mathbf{w}^P and \mathbf{w}^k trained exclusively on group k 's data P_k , with probability at least $1 - \delta$ with $\delta \in (0, 1)$, then the upper bound of risk disparity is*

$$\mathcal{R}_{Q_k}(\mathbf{w}^P) - \mathcal{R}_Q(\mathbf{w}^P) \leq \underbrace{G_k \cdot \text{dist}(\mathcal{P}_k, \mathcal{Q}_k) + G_P \cdot \text{dist}(\mathcal{P}, \mathcal{Q})}_{\text{distribution shift}} + \underbrace{4L^2 G^2 \cdot \text{dist}(\mathcal{P}_k, P)^2 + \Upsilon}_{\text{group gap}} \quad (8)$$

where

$$\Upsilon = \sqrt{\frac{\log(4/\delta)}{2|P|}} + \sqrt{\frac{\log(4/\delta)}{2|P_k|}} + \varpi + \varpi_k.$$

Note that $\mathbb{E}_{z \sim \pi_i}[\ell(\mathbf{w}^k, z)] \leq G_k$, $\varpi = \mathcal{R}_P(\mathbf{w}^P) - \mathcal{R}_Q^*(\mathbf{w}^Q)$ and $\varpi_k = \mathcal{R}_{P_k}(\mathbf{w}^k) - \mathcal{R}_{Q_k}^*(\mathbf{w}^{Q_k})$. ϖ and ϖ_k can be regarded as constants because $\mathcal{R}_P(\mathbf{w}^P)$ and $\mathcal{R}_{P_k}(\mathbf{w}^k)$ correspond to the empirical risks, $\mathcal{R}_Q^*(\mathbf{w}^Q)$ and $\mathcal{R}_{Q_k}^*(\mathbf{w}^{Q_k})$ represent the ideal minimal empirical risk of model \mathbf{w}^Q trained on distribution \mathcal{Q} and \mathcal{Q}_k , respectively.

Interpretations of Theorem 5.2 Eq. (8) illustrates several aspects that induce unfairness. (1) *Group biased data*. For group-level fairness, the more balanced the data is, the smaller the risk disparity would be; (2) *distribution shift*. For source/target distribution, the closer the distributions are, the smaller the performance gap would be; (3) *Data size*. For training data size, a larger data size (potentially eliminating data bias across groups) would lead to a smaller performance gap.

Main observation Theorem 5.1 underscores how the generalization error is impacted by distribution shifts. Theorem 5.2 implies that the risk disparity is essentially influenced by the distribution shift and the inherent group gap term. In practice, approaches that mitigate the group gap, such as imposing fairness regularizers, acquiring new data, or reweight the training data samples [Kamiran and Calders, 2012], will inevitably incur additional distribution shifts between the training and test data. The incurred distribution shift further leads to a performance drop due to the generalization error in Theorem 5.1. Nonetheless, one theoretical insight is that if one can control the negative impacts of potential distribution shifts through generalization error while implementing fairness-enhancing strategies, it is possible to achieve the goal of improving fairness without causing harm. This high-level insight supports the effectiveness of our proposed sampling approach, in which we acquire new data to reduce the group gap through fairness components while preventing the potential adverse impacts of distribution shifts using the accuracy influence component.

6 Empirical Results

In this section, we empirically demonstrate the disparate impact across groups and present the effectiveness of the proposed Fair Influential Sampling method to mitigate the disparity.

6.1 Experimental Setup

We evaluate the performance of our algorithm on four real-world datasets across three different modalities: CelebA [Liu et al., 2015], UCI Adult [Asuncion and Newman, 2007] and Compas [Angwin et al., 2016]. We implement the fairness loss $\phi(\cdot)$ based on three common group fairness metrics: difference of demographic parity (DP), difference of equality of opportunity (EOp), and difference of equal odds (E0d). We compare our method with five baselines: 1) Base (ERM): directly train the model on the training dataset P ; 2) Random: train the model on dataset P and randomly sampled data from U with inquired true labels; 3) BALD [Branchaud-Charron et al., 2021]: active sampling according to the mutual information; 4) ISAL [Liu et al., 2021a]: selects unlabeled examples based on the calculated influence in an active learning setting. We apply model predictions as pseudo-labels; 5) Just Train Twice (JTT) [Liu et al., 2021b]: reweighting those misclassified examples for re-training. Here, we examine a weight of 20 for misclassified examples, marked as JTT-20. Recall that we present the average result of the classifier \mathbf{w}_t outputs from Algorithm 1. More details on datasets and hyper-parameters are provided in Appendix E.

6.2 Main Results

Note that all the experimental results presented subsequently are from three separate trials, each conducted with distinct random seeds. Due to space limits, we provide a full version of the experimental results (tables) in the Appendix E.

Results on image datasets Initially, we train a vision transformer using a patch size of $(8, 8)$ on the CelebA face attribute dataset [Liu et al., 2015]. We select four binary classification targets, including *Smiling*, *Attractive*, *Young*, and *Big Nose*. The sensitive attribute is gender. 2% of the labeled data is allocated for training, while the remaining 98% is reserved for sampling purposes. Then, 10% of the test data is randomly set aside as a hold-out validation set. For ease of computation, only the last two layers of the model are used to calculate the influence of accuracy and fairness components. For Table 1, one main observation is that FIS outperforms baselines with a significant margin on three fairness metrics while maintaining the same accuracy level. This improvement, as indicated in Theorem 5.2, can be attributed to FIS assigning priority to new examples based on the fairness influence, then avoiding accuracy reduction via their accuracy influence.

Results on tabular datasets Next, we work with multi-layer perceptron (MLP) with two layers trained on the Adult [Asuncion and Newman, 2007] and Compas dataset [Angwin et al., 2016], respectively. We select *age* as the sensitive attribute for the Adult dataset and *race* for the Compas dataset. For two datasets, we resample the data to balance the class and group membership [Chawla et al., 2002]. The whole dataset is split into training and test sets at a 4:1 ratio. Then, we randomly re-select 20% of the training set for initial training and the remaining 80% for sampling. Also, 20% examples of the test set are selected to form a validation set. We utilize the whole model parameters to compute the influence of accuracy and fairness for examples. Table 1 summarizes the main results of the Adult and Compas datasets. On the Adult dataset, we observe that our sampling method achieves the lowest violation for equality of opportunity and has a comparable performance for the DP metric. Besides, our algorithm achieves a much better accuracy-fairness trade-off than other baselines on the Compas dataset. JTT-20 achieves a lower fairness violation with the price of a significant accuracy drop compared to other baselines.

6.3 Ablation Study

What is the impact of label budgets? Here, we examine how the varying label budgets r affect the trade-off between accuracy and fairness. For ease of comparison, we adhere to a consistent label budget per round to illustrate their respective impacts. As shown in Figure 2, our method consistently preserves a lower fairness violation than the BALD and ISAL baselines with a similar test accuracy. While we observe that the JTT-20 algorithm can achieve a near-zero fairness violation under a limited budget on the CelebA dataset, we argue that the model accuracy is rather uninformative (about 50%).

How does the hold-out set size affect the performance? We further explore the impact of adjusting the validation set size on our algorithm’s performance. We present the test accuracy and fairness violations across different validation set sizes on the CelebA dataset. Note that the default validation set size is set to 1% of the whole dataset size. In particular, the minimum scale of the validation set size is set to $1/5 \times$ (nearly 400 CelebA images). The results in Figure. 2 indicate that our algorithm still retains the test accuracy and fairness violation when we vary the validation set size.

Table 1: Results of (test_accuracy, fairnessViolation) on **CelebA**, **Adult** and **Compas**. CelebA: Four binary targets: Smiling, Attractive, Young, and Big_Nose; Sensitive attribute: gender. Adult: Binary target: Income; Sensitive attribute: Age. Compas: Binary target: Recidivism; Sensitive attribute: Race. We highlight all results that are fairer without worsening accuracy in **boldface** compared to random sampling. The values after \pm are the standard deviation.

$\epsilon = 0.05$	DP	EOP	DP	EOP	
	CelebA - Smiling			CelebA - Attractive	
Base(ERM)	(0.789 \pm 0.003, 0.127 \pm 0.007)	(0.789 \pm 0.003, 0.067 \pm 0.003)	(0.664 \pm 0.005, 0.251 \pm 0.022)	(0.658 \pm 0.009, 0.179 \pm 0.014)	
Random	(0.837 \pm 0.017, 0.133 \pm 0.001)	(0.840 \pm 0.020, 0.059 \pm 0.005)	(0.693 \pm 0.002, 0.372 \pm 0.006)	(0.693 \pm 0.012, 0.250 \pm 0.011)	
BALD	(0.856 \pm 0.024, 0.140 \pm 0.012)	(0.854 \pm 0.025, 0.062 \pm 0.005)	(0.712 \pm 0.015, 0.431 \pm 0.020)	(0.712 \pm 0.016, 0.297 \pm 0.008)	
ISAL	(0.867 \pm 0.022, 0.138 \pm 0.010)	(0.867 \pm 0.022, 0.057 \pm 0.007)	(0.713 \pm 0.009, 0.410 \pm 0.003)	(0.713 \pm 0.009, 0.275 \pm 0.011)	
JTT-20	(0.698 \pm 0.018, 0.077 \pm 0.006)	(0.679 \pm 0.013, 0.045 \pm 0.002)	(0.621 \pm 0.015, 0.094 \pm 0.004)	(0.605 \pm 0.013, 0.083 \pm 0.011)	
FIS	(0.848\pm0.025, 0.084\pm0.055)	(0.845\pm0.034, 0.032\pm0.007)	(0.658 \pm 0.016, 0.217 \pm 0.048)	(0.674\pm0.015, 0.112\pm0.025)	
	CelebA - Young			CelebA - Big_Nose	
Base(ERM)	(0.755 \pm 0.002, 0.190 \pm 0.017)	(0.759 \pm 0.005, 0.102 \pm 0.005)	(0.752 \pm 0.024, 0.198 \pm 0.034)	(0.755 \pm 0.022, 0.206 \pm 0.018)	
Random	(0.763 \pm 0.008, 0.158 \pm 0.016)	(0.698 \pm 0.109, 0.075 \pm 0.021)	(0.760 \pm 0.009, 0.177 \pm 0.014)	(0.757 \pm 0.004, 0.190 \pm 0.029)	
BALD	(0.776 \pm 0.021, 0.165 \pm 0.019)	(0.775 \pm 0.020, 0.076 \pm 0.007)	(0.777 \pm 0.004, 0.184 \pm 0.016)	(0.765 \pm 0.003, 0.209 \pm 0.014)	
ISAL	(0.781 \pm 0.020, 0.180 \pm 0.014)	(0.781 \pm 0.020, 0.084 \pm 0.006)	(0.782\pm0.001, 0.148\pm0.059)	(0.782\pm0.001, 0.154\pm0.080)	
JTT-20	(0.774 \pm 0.026, 0.167 \pm 0.016)	(0.774 \pm 0.024, 0.083 \pm 0.007)	(0.771 \pm 0.014, 0.191 \pm 0.036)	(0.758 \pm 0.026, 0.223 \pm 0.018)	
FIS	(0.763\pm0.004, 0.104\pm0.059)	(0.773\pm0.003, 0.041\pm0.015)	(0.779\pm0.009, 0.089\pm0.076)	(0.780\pm0.013, 0.046\pm0.072)	
	Adult - Income			Compas - Recidivism	
Base(ERM)	(0.665 \pm 0.045, 0.255 \pm 0.041)	(0.665 \pm 0.045, 0.115 \pm 0.036)	(0.670 \pm 0.005, 0.333 \pm 0.008)	(0.675 \pm 0.005, 0.267 \pm 0.010)	
Random	(0.765 \pm 0.021, 0.209 \pm 0.042)	(0.758 \pm 0.027, 0.127 \pm 0.013)	(0.689 \pm 0.007, 0.305 \pm 0.023)	(0.686 \pm 0.016, 0.253 \pm 0.035)	
BALD	(0.767\pm0.019, 0.203\pm0.017)	(0.703 \pm 0.111, 0.117 \pm 0.013)	(0.688 \pm 0.011, 0.313 \pm 0.012)	(0.686 \pm 0.015, 0.256 \pm 0.031)	
ISAL	(0.765 \pm 0.020, 0.215 \pm 0.011)	(0.755 \pm 0.028, 0.128 \pm 0.013)	(0.697 \pm 0.002, 0.308 \pm 0.025)	(0.698 \pm 0.004, 0.274 \pm 0.022)	
JTT-20	(0.751 \pm 0.013, 0.262 \pm 0.020)	(0.742 \pm 0.018, 0.149 \pm 0.021)	(0.646 \pm 0.009, 0.240 \pm 0.016)	(0.630 \pm 0.024, 0.141 \pm 0.028)	
FIS	(0.766 \pm 0.013, 0.214 \pm 0.009)	(0.757\pm0.034, 0.113\pm0.017)	(0.690\pm0.002, 0.299\pm0.029)	(0.694\pm0.002, 0.241\pm0.035)	

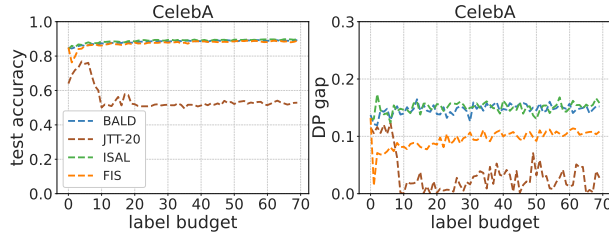


Figure 2: **Left:** The impact of label budgets on the test accuracy & DP gap in the **CelebA** dataset. **Right:** The impact of the hold-out set size on (test_accuracy, fairnessViolation) results.

7 Conclusions and Limitations

In this work, we are interested in facilitating ML models that mitigate group fairness disparity without harming model accuracy. To achieve this, different from current active sampling methods, we propose a tractable fair influential sampling method FIS, which avoids the need for training group annotations during the sampling or training phase, thereby preventing the potential exposure of sensitive information. In particular, this algorithm acquires data samples from a large dataset for training based on the influence of fairness and accuracy evaluated on the auxiliary validation dataset. Empirical experiments on real-world data validate the efficacy of our proposed method. Nonetheless, we recognize that our method has limitations. Although the proposed sampling algorithm does not require sensitive attribute information from the massive data, it relies on a clean and informative validation set that contains the sensitive attributes of data examples. We consider this as a reasonable requirement in practice, given the relatively modest size of the validation set.

Broader Impact

This paper presents work whose goal is to advance the field of fairness in machine learning. There are many potential societal consequences of our work. While the proposed algorithm does intend to infer sensitive attributes of data examples that may be protected by privacy regulations, it does not necessitate direct access to such sensitive information. On the other hand, our work can serve as an effective approach leading to mitigating the disparity with a limited annotation budget. We have thoroughly examined the potential ethical implications of our work and, based on our assessment, do not identify any issues that we deem necessary to emphasize here specifically.

References

Naeem Siddiqi. Credit risk scorecards: Developing and implementing intelligent credit scoring. 2005.

Réal André Carbonneau, Kevin Laframboise, and Rustam M. Vahidov. Application of machine learning techniques for supply chain demand forecasting. *Eur. J. Oper. Res.*, 184:1140–1154, 2008.

Zhaowei Zhu, Yuanshun Yao, Jiankai Sun, Hang Li, and Yang Liu. Weak proxies are sufficient and preferable for fairness with missing sensitive attributes. In *International Conference on Machine Learning*, pages 43258–43288. PMLR, 2023.

Aditya Krishna Menon and Robert C Williamson. The cost of fairness in binary classification. In *Conference on Fairness, accountability and transparency*, pages 107–118. PMLR, 2018.

Sanghamitra Dutta, Dennis Wei, Hazar Yueksel, Pin-Yu Chen, Sijia Liu, and Kush Varshney. Is there a trade-off between fairness and accuracy? a perspective using mismatched hypothesis testing. In *International conference on machine learning*, pages 2803–2813. PMLR, 2020.

Han Zhao and Geoffrey J Gordon. Inherent tradeoffs in learning fair representations. *The Journal of Machine Learning Research*, 23(1):2527–2552, 2022.

Jialu Wang, Xin Eric Wang, and Yang Liu. Understanding instance-level impact of fairness constraints. In *International Conference on Machine Learning*, pages 23114–23130. PMLR, 2022a.

Zhaowei Zhu, Tianyi Luo, and Yang Liu. The rich get richer: Disparate impact of semi-supervised learning. *arXiv preprint arXiv:2110.06282*, 2021.

Yuyan Wang, Xuezhi Wang, Alex Beutel, Flavien Prost, Jilin Chen, and Ed H Chi. Understanding and improving fairness-accuracy trade-offs in multi-task learning. In *Proceedings of the 27th ACM SIGKDD Conference on Knowledge Discovery & Data Mining*, pages 1748–1757, 2021a.

Natalia Martinez, Martin Bertran, and Guillermo Sapiro. Minimax pareto fairness: A multi objective perspective. In *International conference on machine learning*, pages 6755–6764. PMLR, 2020.

Ananth Balashankar, Alyssa Lees, Chris Welty, and Lakshminarayanan Subramanian. What is fair? exploring pareto-efficiency for fairness constrained classifiers. *arXiv preprint arXiv:1910.14120*, 2019.

Susan Wei and Marc Niethammer. The fairness-accuracy pareto front. *Statistical Analysis and Data Mining: The ASA Data Science Journal*, 15(3):287–302, 2022.

Pareto efficiency and production possibility frontier. https://en.wikipedia.org/wiki/Production%20possibility_frontier.

Richard G Lipsey. An introduction to positive economics-4. 1975.

Hadi Anahideh, Abolfazl Asudeh, and Saravanan Thirumuruganathan. Fair active learning. *Expert Systems with Applications*, 199:116981, 2022.

Kenneth Holstein, Jennifer Wortman Vaughan, Hal Daumé III, Miro Dudik, and Hanna Wallach. Improving fairness in machine learning systems: What do industry practitioners need? In *Proceedings of the 2019 CHI conference on human factors in computing systems*, pages 1–16, 2019.

McKane Andrus, Elena Spitzer, Jeffrey Brown, and Alice Xiang. What we can't measure, we can't understand: Challenges to demographic data procurement in the pursuit of fairness. In *Proceedings of the 2021 ACM conference on fairness, accountability, and transparency*, pages 249–260, 2021.

Michael Veale and Reuben Binns. Fairer machine learning in the real world: Mitigating discrimination without collecting sensitive data. *Big Data & Society*, 4(2):2053951717743530, 2017.

Michele Donini, Luca Oneto, Shai Ben-David, John S Shawe-Taylor, and Massimiliano Pontil. Empirical risk minimization under fairness constraints. *Advances in neural information processing systems*, 31, 2018.

Moritz Hardt, Eric Price, and Nati Srebro. Equality of opportunity in supervised learning. *Advances in neural information processing systems*, 29, 2016.

Alekh Agarwal, Alina Beygelzimer, Miroslav Dudík, John Langford, and Hanna Wallach. A reductions approach to fair classification. In *Proceedings of the 35th International Conference on Machine Learning (ICML '18)*, 2018.

Muhammad Bilal Zafar, Isabel Valera, Manuel Gomez Rodriguez, and Krishna P Gummadi. Fairness constraints: Mechanisms for fair classification. In *Proceedings of the 20th International Conference on Artificial Intelligence and Statistics (AISTATS)*, 2017.

Yatong Chen, Reilly Raab, Jialu Wang, and Yang Liu. Fairness transferability subject to bounded distribution shift. *Advances in Neural Information Processing Systems*, 35:11266–11278, 2022.

Flavien Prost, Hai Qian, Qiuwen Chen, Ed H Chi, Jilin Chen, and Alex Beutel. Toward a better trade-off between performance and fairness with kernel-based distribution matching. *arXiv preprint arXiv:1910.11779*, 2019.

Peizhao Li and Hongfu Liu. Achieving fairness at no utility cost via data reweighing with influence. In *International Conference on Machine Learning*, pages 12917–12930. PMLR, 2022.

David D Lewis and Jason Catlett. Heterogeneous uncertainty sampling for supervised learning. In *Machine learning proceedings 1994*, pages 148–156. Elsevier, 1994.

Michael Lindenbaum, Shaul Markovitch, and Dmitry Rusakov. Selective sampling for nearest neighbor classifiers. *Machine learning*, 54:125–152, 2004.

Sanjoy Dasgupta and Daniel Hsu. Hierarchical sampling for active learning. In *Proceedings of the 25th international conference on Machine learning*, pages 208–215, 2008.

Ran Wang, Sam Kwong, and Degang Chen. Inconsistency-based active learning for support vector machines. *Pattern Recognition*, 45(10):3751–3767, 2012.

Steven CH Hoi, Rong Jin, and Michael R Lyu. Large-scale text categorization by batch mode active learning. In *Proceedings of the 15th international conference on World Wide Web*, pages 633–642, 2006.

Nicholas Roy and Andrew McCallum. Toward optimal active learning through monte carlo estimation of error reduction. *ICML, Williamstown*, 2:441–448, 2001.

Zhuoming Liu, Hao Ding, Huaping Zhong, Weijia Li, Jifeng Dai, and Conghui He. Influence selection for active learning. In *Proceedings of the IEEE/CVF International Conference on Computer Vision*, pages 9274–9283, 2021a.

Tianyang Wang, Xingjian Li, Pengkun Yang, Guosheng Hu, Xiangrui Zeng, Siyu Huang, Cheng-Zhong Xu, and Min Xu. Boosting active learning via improving test performance. In *Proceedings of the AAAI Conference on Artificial Intelligence*, volume 36, pages 8566–8574, 2022b.

Zayd Hammoudeh and Daniel Lowd. Training data influence analysis and estimation: A survey. *arXiv preprint arXiv:2212.04612*, 2022.

Yichen Xie, Han Lu, Junchi Yan, Xiaokang Yang, Masayoshi Tomizuka, and Wei Zhan. Active finetuning: Exploiting annotation budget in the pretraining-finetuning paradigm. In *Proceedings of the IEEE/CVF Conference on Computer Vision and Pattern Recognition*, pages 23715–23724, 2023.

Tatsunori Hashimoto, Megha Srivastava, Hongseok Namkoong, and Percy Liang. Fairness without demographics in repeated loss minimization. In *International Conference on Machine Learning*, pages 1929–1938. PMLR, 2018.

Polina Kirichenko, Pavel Izmailov, and Andrew Gordon Wilson. Last layer re-training is sufficient for robustness to spurious correlations. *arXiv preprint arXiv:2204.02937*, 2022.

Evan Z Liu, Behzad Haghgoo, Annie S Chen, Aditi Raghunathan, Pang Wei Koh, Shiori Sagawa, Percy Liang, and Chelsea Finn. Just train twice: Improving group robustness without training group information. In *International Conference on Machine Learning*, pages 6781–6792. PMLR, 2021b.

Preethi Lahoti, Alex Beutel, Jilin Chen, Kang Lee, Flavien Prost, Nithum Thain, Xuezhi Wang, and Ed Chi. Fairness without demographics through adversarially reweighted learning. *Advances in neural information processing systems*, 33:728–740, 2020.

Akshaj Kumar Veldanda, Ivan Brugere, Sanghamitra Dutta, Alan Mishler, and Siddharth Garg. Hyper-parameter tuning for fair classification without sensitive attribute access. *arXiv preprint arXiv:2302.01385*, 2023.

Nimit Sohoni, Jared Dunnmon, Geoffrey Angus, Albert Gu, and Christopher Ré. No subclass left behind: Fine-grained robustness in coarse-grained classification problems. *Advances in Neural Information Processing Systems*, 33:19339–19352, 2020.

Abolfazl Asudeh, Zhongjun Jin, and HV Jagadish. Assessing and remedying coverage for a given dataset. In *2019 IEEE 35th International Conference on Data Engineering (ICDE)*, pages 554–565. IEEE, 2019.

Fabio Azzalini, Chiara Criscuolo, and Letizia Tanca. Fair-db: Functional dependencies to discover data bias. In *EDBT/ICDT Workshops*, 2021.

Ki Hyun Tae and Steven Euijong Whang. Slice tuner: A selective data acquisition framework for accurate and fair machine learning models. In *Proceedings of the 2021 International Conference on Management of Data*, pages 1771–1783, 2021.

Shubham Sharma, Yunfeng Zhang, Jesús M Ríos Aliaga, Djallel Bouneffouf, Vinod Muthusamy, and Kush R Varshney. Data augmentation for discrimination prevention and bias disambiguation. In *Proceedings of the AAAI/ACM Conference on AI, Ethics, and Society*, pages 358–364, 2020.

L Elisa Celis, Vijay Keswani, and Nisheeth Vishnoi. Data preprocessing to mitigate bias: A maximum entropy based approach. In *International conference on machine learning*, pages 1349–1359. PMLR, 2020.

Nitesh V Chawla, Kevin W Bowyer, Lawrence O Hall, and W Philip Kegelmeyer. Smote: synthetic minority over-sampling technique. *Journal of artificial intelligence research*, 16:321–357, 2002.

Rich Zemel, Yu Wu, Kevin Swersky, Toni Pitassi, and Cynthia Dwork. Learning fair representations. In *International conference on machine learning*, pages 325–333. PMLR, 2013.

Irene Chen, Fredrik D Johansson, and David Sontag. Why is my classifier discriminatory? *Advances in neural information processing systems*, 31, 2018.

Jialu Wang, Yang Liu, and Caleb Levy. Fair classification with group-dependent label noise. In *Proceedings of the 2021 ACM Conference on Fairness, Accountability, and Transparency, FAccT '21*, page 526–536, New York, NY, USA, 2021b. Association for Computing Machinery. ISBN 9781450383097. doi: 10.1145/3442188.3445915. URL <https://doi.org/10.1145/3442188.3445915>.

Faisal Kamiran and Toon Calders. Data preprocessing techniques for classification without discrimination. *Knowledge and information systems*, 33(1):1–33, 2012.

Heinrich Jiang and Ofir Nachum. Identifying and correcting label bias in machine learning. In *International Conference on Artificial Intelligence and Statistics*, pages 702–712. PMLR, 2020.

Maurice Diesendruck, Ethan R Elenberg, Rajat Sen, Guy W Cole, Sanjay Shakkottai, and Sinead A Williamson. Importance weighted generative networks. In *Machine Learning and Knowledge Discovery in Databases: European Conference, ECML PKDD 2019, Würzburg, Germany, September 16–20, 2019, Proceedings, Part II*, pages 249–265. Springer, 2020.

Kristy Choi, Aditya Grover, Trisha Singh, Rui Shu, and Stefano Ermon. Fair generative modeling via weak supervision. In *International Conference on Machine Learning*, pages 1887–1898. PMLR, 2020.

Maan Qraitem, Kate Saenko, and Bryan A Plummer. Bias mimicking: A simple sampling approach for bias mitigation. In *Proceedings of the IEEE/CVF Conference on Computer Vision and Pattern Recognition*, pages 20311–20320, 2023.

Yi Li and Nuno Vasconcelos. Repair: Removing representation bias by dataset resampling. In *Proceedings of the IEEE/CVF conference on computer vision and pattern recognition*, pages 9572–9581, 2019.

Michael Feldman. *Computational fairness: Preventing machine-learned discrimination*. PhD thesis, 2015.

Michael Feldman, Sorelle A Friedler, John Moeller, Carlos Scheidegger, and Suresh Venkatasubramanian. Certifying and removing disparate impact. In *proceedings of the 21th ACM SIGKDD international conference on knowledge discovery and data mining*, pages 259–268, 2015.

Blake Woodworth, Suriya Gunasekar, Mesrob I Ohannessian, and Nathan Srebro. Learning non-discriminatory predictors. In *Conference on Learning Theory*, pages 1920–1953. PMLR, 2017.

Geoff Pleiss, Manish Raghavan, Felix Wu, Jon Kleinberg, and Kilian Q Weinberger. On fairness and calibration. In *Advances in Neural Information Processing Systems*, pages 5680–5689, 2017.

Wenlong Chen, Yegor Klochkov, and Yang Liu. Post-hoc bias scoring is optimal for fair classification. *arXiv preprint arXiv:2310.05725*, 2023.

Muhammad Bilal Zafar, Isabel Valera, Manuel Gomez-Rodriguez, and Krishna P Gummadi. Fairness constraints: A flexible approach for fair classification. *The Journal of Machine Learning Research*, 20(1):2737–2778, 2019.

Alekh Agarwal, Miroslav Dudík, and Zhiwei Steven Wu. Fair regression: Quantitative definitions and reduction-based algorithms. In *International Conference on Machine Learning*, pages 120–129. PMLR, 2019.

Joy Buolamwini and Timnit Gebru. Gender shades: Intersectional accuracy disparities in commercial gender classification. In *Conference on fairness, accountability and transparency*, pages 77–91. PMLR, 2018.

Changjian Shui, Gezheng Xu, Qi Chen, Jiaqi Li, Charles X Ling, Tal Arbel, Boyu Wang, and Christian Gagné. On learning fairness and accuracy on multiple subgroups. *Advances in Neural Information Processing Systems*, 35: 34121–34135, 2022.

Tian Li, Maziar Sanjabi, Ahmad Beirami, and Virginia Smith. Fair resource allocation in federated learning. In *International Conference on Learning Representations*, 2019.

Natalia Martinez, Martin Bertran, and Guillermo Sapiro. Fairness with minimal harm: A pareto-optimal approach for healthcare. *arXiv preprint arXiv:1911.06935*, 2019.

Pang Wei Koh and Percy Liang. Understanding black-box predictions via influence functions. In *International conference on machine learning*, pages 1885–1894. PMLR, 2017.

Vitaly Feldman. Does learning require memorization? a short tale about a long tail. In *Proceedings of the 52nd Annual ACM SIGACT Symposium on Theory of Computing*, pages 954–959, 2020.

Ziwei Liu, Ping Luo, Xiaogang Wang, and Xiaoou Tang. Deep learning face attributes in the wild. In *Proceedings of the IEEE international conference on computer vision*, pages 3730–3738, 2015.

Arthur Asuncion and David Newman. Uci machine learning repository, 2007.

Julia Angwin, Jeff Larson, Surya Mattu, and Lauren Kirchner. Machine bias. 2016.

Frédéric Branchaud-Charron, Parmida Atighehchian, Pau Rodríguez, Grace Abuhamad, and Alexandre Lacoste. Can active learning preemptively mitigate fairness issues? *arXiv preprint arXiv:2104.06879*, 2021.

Harvineet Singh, Rina Singh, Vishwali Mhasawade, and Rumi Chunara. Fairness violations and mitigation under covariate shift. In *Proceedings of the 2021 ACM Conference on Fairness, Accountability, and Transparency*, pages 3–13, 2021.

Yuji Roh, Kangwook Lee, Steven Euijong Whang, and Changho Suh. Improving fair training under correlation shifts. *arXiv preprint arXiv:2302.02323*, 2023.

Stephen Giguere, Blossom Metevier, Yuriy Brun, Bruno Castro da Silva, Philip S Thomas, and Scott Niekum. Fairness guarantees under demographic shift. In *Proceedings of the 10th International Conference on Learning Representations (ICLR)*, 2022.

Solon Barocas, Moritz Hardt, and Arvind Narayanan. *Fairness and machine learning: Limitations and opportunities*. MIT Press, 2023.

Appendix

The Appendix is organized as follows.

- Section A provides more details of the related work.
- Section B explores the relationship between our proposed fairness notion risk disparity and common fairness metrics, such as DP and EOd. In particular, we provide the full proof for Proposition 3.1.
- Section C provides a detailed analysis of the FIS algorithm including 1) evaluating first-order influence estimations against real influence, 2) a comparative analysis of computational costs, and 3) the exploration of the labeling strategies.
- Section D presents the full proofs for the Lemmas and Theorems shown in Section 4 and Section 5.
- Section E presents detailed descriptions of all datasets, corresponding parameter settings, and full version of the experimental results.

A More Details of Related Work

Active learning The core idea of active learning is to rank unlabeled instances by developing specific significant measures, including uncertainty [Lewis and Catlett, 1994, Lindenbaum et al., 2004], representativeness [Dasgupta and Hsu, 2008], inconsistency [Wang et al., 2012], variance [Hoi et al., 2006], and error [Roy and McCallum, 2001]. Each of these measures has its criterion to determine the importance of instances for enhancing classifier performance. For example, uncertainty considers the most important unlabeled instance to be the nearest one to the current classification boundary. A related line of work [Liu et al., 2021a, Wang et al., 2022b, Hammoudeh and Lowd, 2022, Xie et al., 2023] concentrates on ranking unlabeled instances based on the influence function. Compared to these studies with a focus on prediction accuracy, our work poses a distinct challenge taking into account fairness violations. We note that adopting a particular sampling strategy can lead to distribution shifts between the training and testing data. What's worse, even though fairness is satisfied within the training dataset, the model may still exhibit unfair treatments on the test dataset due to the distribution shift. Therefore, it becomes imperative for the sampling approach to also account for its potential impacts on fairness.

Pareto optimality In the field of fairness in machine learning, Pareto optimality indicates the theoretical frontier of fairness accuracy tradeoff, meaning that fairness can not be improved without worsening model accuracy. Existing methods primarily focus on seeking the Pareto frontier of fairness accuracy tradeoff for the neural network classifier, instead of reaching a better one. For example, Balashankar et al. [2019] first analyzes the Pareto optimality for classifiers within the context of fairness constraints. Wang et al. [2021a] explores the multi-dimensional Pareto frontiers of the fairness-accuracy tradeoff in the multi-task setting. Martinez et al. [2020, 2019] target to obtain a Pareto efficient classifier to reduce worst-case group risks by formulating group fairness as a multiple-objective optimization problem, where each group risk is an objective function.

Fair classification The fairness-aware learning algorithms, in general, can be categorized into pre-processing, in-processing, and post-processing methods. Pre-processing methods typically reweigh or distort the data examples to mitigate the identified biases [Asudeh et al., 2019, Azzalini et al., 2021, Tae and Whang, 2021, Sharma et al., 2020, Celis et al., 2020, Chawla et al., 2002, Zemel et al., 2013, Chen et al., 2018]. More relevant to us is the *importance reweighting*, which assigns different weights to different training examples to ensure fairness across groups [Kamiran and Calders, 2012, Jiang and Nachum, 2020, Diesendruck et al., 2020, Choi et al., 2020, Qraitem et al., 2023, Li and Vasconcelos, 2019]. Our proposed algorithm bears similarity to a specific case of importance reweighting, particularly the 0-1 reweighting applied to newly added data. The main advantage of our work, however, lies in its ability to operate without needing access to the sensitive attributes of either the new or training data. Other parallel studies utilize importance weighting to learn a complex fair generative model in a weakly supervised setting [Diesendruck et al., 2020, Choi et al., 2020], or to mitigate representation bias in training datasets [Li and Vasconcelos, 2019]. Post-processing methods typically enforce fairness on a learned model through calibration [Feldman, 2015, Feldman et al., 2015, Hardt et al., 2016]. Although this approach is likely to decrease the disparity of the classifier, by decoupling the training from the fairness enforcement, this procedure may not lead to the best trade-off between fairness and accuracy [Woodworth et al., 2017, Pleiss et al., 2017]. In contrast, our work can achieve a better trade-off between fairness and accuracy, because we reduce the fairness disparity by mitigating the adverse effects of distribution shifts on generalization error. Additionally, these post-processing techniques necessitate access to the sensitive attribute during the inference phase, which is often not available in many real-world scenarios.

Fairness-accuracy tradeoff It has been demonstrated that there is an implicit trade-off between fairness and accuracy in the literature. Compared to the prior works [Menon and Williamson, 2018, Prost et al., 2019], our work does not require additional assumptions about the classifier and the characteristics of the training/testing datasets (for example,

distribution shifts). Besides, the main difference is that our paper does not work in the classical regime of the fairness-accuracy tradeoff. By properly collecting new data from an unlabeled dataset, we can improve both generalization and fairness at the same time, which cannot be achieved by working on a fixed and static training dataset that naturally incurs such a tradeoff. Recent work Li and Liu [2022] utilizes the influence function to reweight the data examples but requires re-training. Our method focuses on soliciting additional samples from an external unlabeled dataset while [Li and Liu, 2022] reweights the existing and fixed training dataset.

Fair classifiers without demographics Common research concerning distribution shifts necessitates extra assumptions to build theoretical connections between features and attributes, like causal graphs [Singh et al., 2021], correlation shifts [Roh et al., 2023], and demographic shifts [Giguere et al., 2022]. In contrast, our approach refrains from making further assumptions about the properties of distribution shifts. In this literature, many works have utilized distributionally robust optimization (DRO) to reduce fairness disparity without sensitive attribute information [Hashimoto et al., 2018, Kirichenko et al., 2022, Liu et al., 2021b, Lahoti et al., 2020, Veldanda et al., 2023, Sohoni et al., 2020]. Although these works also evaluate the worst-group performance in the context of fairness, their approach differs as they do not strive to equalize the loss across all groups. Besides, in these studies, accuracy and worst-case accuracy are used to showcase the efficacy of DRO. Essentially, they equate fairness with uniform accuracy across groups, implying a model is considered fair if it demonstrates equal accuracies for all groups. However, this specific definition of fairness is somewhat restrictive and does not align with more conventional fairness definitions like DP or EOD.

B Understanding Risk Disparity Through Fairness Metrics

Here, we provide a brief proof to illustrate Proposition 3.1, that is, the relationship between risk parity and common fairness metrics, such as DP and EOD.

Proposition 3.1. Consider a binary classification scenario involving two demographic groups. When two groups are balanced, i.e., $\frac{\mathbb{P}(Y=y|S=k)}{\mathbb{P}(Y=y|S=k')} = 1$, risk disparity can serve as a lower bound for fairness disparities based on EOD. Similarly, if the group sufficiency ratio can be calibrated by 1, i.e., $\mathbb{P}(Y = y|S = k, \hat{Y} = y) = \mathbb{P}(Y = y|S = k', \hat{Y} = y) = R$ where R is calibration score, risk disparity can be formulated as a lower bound for DP-based fairness disparity.

Proof. Consider a scenario involving two demographic groups $S \in \{k, k'\}$, alongside a 0-1 loss function.

Fairness Metric EOd For EOd, the risk disparity can be reformulated as

$$\begin{aligned}
& |\mathcal{R}_{Q_k}(\mathbf{w}^P) - \mathcal{R}_{Q_{k'}}(\mathbf{w}^P)| \\
&= \left| \frac{1}{|Q_k|} \sum_{(x_n, y_n) \in Q_k} \mathbb{I}(\hat{y}_n \neq y_n) - \frac{1}{|Q_{k'}|} \sum_{(x_n, y_n) \in Q_{k'}} \mathbb{I}(\hat{y}_n \neq y_n) \right| \\
&= \left| \mathbb{P}(\hat{Y} \neq Y \mid S = k) - \mathbb{P}(\hat{Y} \neq Y \mid S = k') \right| \\
&= \left| \sum_y \left(\mathbb{P}(Y = y \mid S = k') \mathbb{P}(\hat{Y} = y \mid S = k', Y = y) - \mathbb{P}(Y = y \mid S = k) \mathbb{P}(\hat{Y} = y \mid S = k, Y = y) \right) \right| \\
&= \left| \sum_y \mathbb{P}(Y = y \mid S = k') \cdot \left(\mathbb{P}(\hat{Y} = y \mid S = k', Y = y) - \omega_{\text{EOd}}(y) \mathbb{P}(\hat{Y} = y \mid S = k, Y = y) \right) \right| \\
&= \left| \mathbb{P}(Y = 1 \mid S = k') \cdot \left(\mathbb{P}(\hat{Y} = 1 \mid S = k', Y = 1) - \omega_{\text{EOd}}(y = 1) \cdot \mathbb{P}(\hat{Y} = 1 \mid S = k, Y = 1) \right) \right. \quad \# \text{ binary case} \\
&\quad \left. + \mathbb{P}(Y = 0 \mid S = k') \cdot \left(\mathbb{P}(\hat{Y} = 0 \mid S = k', Y = 0) - \omega_{\text{EOd}}(y = 0) \cdot \mathbb{P}(\hat{Y} = 0 \mid S = k, Y = 0) \right) \right| \\
&= \left| \mathbb{P}(Y = 1 \mid S = k') \cdot \left(\mathbb{P}(\hat{Y} = 1 \mid S = k', Y = 1) - \omega_{\text{EOd}}(y = 1) \cdot \mathbb{P}(\hat{Y} = 1 \mid S = k, Y = 1) \right) \right. \\
&\quad \left. + \mathbb{P}(Y = 0 \mid S = k') \cdot \left(\omega_{\text{EOd}}(y = 0) \cdot \mathbb{P}(\hat{Y} = 1 \mid S = k, Y = 0) - \mathbb{P}(\hat{Y} = 1 \mid S = k', Y = 0) \right) \right. \\
&\quad \left. + \mathbb{P}(Y = 0 \mid S = k') \cdot (1 - \omega_{\text{EOd}}(y = 0)) \right| \\
&= \left| \mathbb{P}(Y = 1 \mid S = k') \cdot \left(\mathbb{P}(\hat{Y} = 1 \mid S = k', Y = 1) - \mathbb{P}(\hat{Y} = 1 \mid S = k, Y = 1) \right) \right. \\
&\quad \left. - \mathbb{P}(Y = 0 \mid S = k') \cdot \left(\mathbb{P}(\hat{Y} = 1 \mid S = k', Y = 0) - \mathbb{P}(\hat{Y} = 1 \mid S = k, Y = 0) \right) \right| \quad \# \text{ balanced groups} \\
&\leq \mathbb{P}(Y = 1 \mid S = k') \cdot \left| \mathbb{P}(\hat{Y} = 1 \mid S = k', Y = 1) - \mathbb{P}(\hat{Y} = 1 \mid S = k, Y = 1) \right| \\
&\quad + \mathbb{P}(Y = 0 \mid S = k') \cdot \left| \mathbb{P}(\hat{Y} = 1 \mid S = k', Y = 0) - \mathbb{P}(\hat{Y} = 1 \mid S = k, Y = 0) \right| \\
&\leq \underbrace{\sum_{y \in \{0, 1\}} \left| \mathbb{P}(\hat{Y} = 1 \mid S = k', Y = y) - \mathbb{P}(\hat{Y} = 1 \mid S = k, Y = y) \right|}_{\text{EOd-based fairness disparity}}
\end{aligned}$$

where we define $\omega_{\text{EOd}}(y) := \frac{\mathbb{P}(Y = y \mid S = k)}{\mathbb{P}(Y = y \mid S = k')}$, serving as the bias weight. Here, we make a mild assumption that the two demographic groups are balanced, i.e., $\omega_{\text{EOd}}(y) = 1$. Then, we can see that the last item measures the fairness disparity based on EOd for binary classification problems. Thus, we can claim that reducing risk disparity can promote the fairness metric EOd.

Fairness Metric DP Similarly, for DP, we formulate the risk disparity as

$$\begin{aligned}
& |\mathcal{R}_{Q_k}(\mathbf{w}^P) - \mathcal{R}_{Q_{k'}}(\mathbf{w}^P)| \\
&= \left| \frac{1}{|Q_k|} \sum_{(x_n, y_n) \in Q_k} \mathbb{I}(\hat{y}_n \neq y_n) - \frac{1}{|Q_{k'}|} \sum_{(x_n, y_n) \in Q_{k'}} \mathbb{I}(\hat{y}_n \neq y_n) \right| \\
&= \left| \mathbb{P}(\hat{Y} \neq Y \mid S = k) - \mathbb{P}(\hat{Y} \neq Y \mid S = k') \right| \\
&= \left| \sum_y \left(\mathbb{P}(\hat{Y} = y \mid S = k') \mathbb{P}(Y = y \mid S = k', \hat{Y} = y) - \mathbb{P}(\hat{Y} = y \mid S = k) \mathbb{P}(Y = y \mid S = k, \hat{Y} = y) \right) \right| \\
&= \left| \sum_y \mathbb{P}(Y = y \mid S = k', \hat{Y} = y) \cdot \left(\mathbb{P}(\hat{Y} = y \mid S = k') - \omega_{\text{DP}}(y) \mathbb{P}(\hat{Y} = y \mid S = k) \right) \right| \\
&= \left| \mathbb{P}(Y = 1 \mid S = k', \hat{Y} = 1) \cdot \left(\mathbb{P}(\hat{Y} = 1 \mid S = k') - \omega_{\text{DP}}(y = 1) \cdot \mathbb{P}(\hat{Y} = 1 \mid S = k) \right) \right. \\
&\quad \left. + \mathbb{P}(Y = 0 \mid S = k', \hat{Y} = 0) \cdot \left(\mathbb{P}(\hat{Y} = 0 \mid S = k') - \omega_{\text{DP}}(y = 0) \cdot \mathbb{P}(\hat{Y} = 0 \mid S = k) \right) \right| \\
&= \left| \mathbb{P}(Y = 1 \mid S = k', \hat{Y} = 1) \cdot \left(\mathbb{P}(\hat{Y} = 1 \mid S = k') - \omega_{\text{DP}}(y = 1) \cdot \mathbb{P}(\hat{Y} = 1 \mid S = k) \right) \right. \\
&\quad \left. + \mathbb{P}(Y = 0 \mid S = k', \hat{Y} = 0) \cdot \left(\omega_{\text{DP}}(y = 0) \cdot \mathbb{P}(\hat{Y} = 1 \mid S = k) - \mathbb{P}(\hat{Y} = 1 \mid S = k') \right) \right. \\
&\quad \left. + \mathbb{P}(Y = 0 \mid S = k', \hat{Y} = 0) \cdot (1 - \omega_{\text{DP}}(y = 0)) \right| \quad \# \text{Calibrating group sufficiency} \\
&= \left| \mathbb{P}(Y = 1 \mid S = k', \hat{Y} = 1) \cdot \left(\mathbb{P}(\hat{Y} = 1 \mid S = k') - \mathbb{P}(\hat{Y} = 1 \mid S = k) \right) \right. \\
&\quad \left. + \mathbb{P}(Y = 0 \mid S = k', \hat{Y} = 0) \cdot \left(\mathbb{P}(\hat{Y} = 1 \mid S = k) - \mathbb{P}(\hat{Y} = 1 \mid S = k') \right) \right| \\
&= \left| \mathbb{P}(Y = 1 \mid S = k', \hat{Y} = 1) - \mathbb{P}(Y = 0 \mid S = k', \hat{Y} = 0) \right| \cdot \left| \mathbb{P}(\hat{Y} = 1 \mid S = k') - \mathbb{P}(\hat{Y} = 1 \mid S = k) \right| \\
&\leq \underbrace{\left| \mathbb{P}(\hat{Y} = 1 \mid S = k') - \mathbb{P}(\hat{Y} = 1 \mid S = k) \right|}_{\text{DP-based fairness disparity}}
\end{aligned}$$

where we define $\omega_{\text{DP}}(y) := \frac{\mathbb{P}(Y=y \mid S=k, \hat{Y}=y)}{\mathbb{P}(Y=y \mid S=k', \hat{Y}=y)}$. In fact, $\omega_{\text{DP}}(y)$ measures the group sufficiency ratio [Shui et al., 2022]. Note that the group sufficiency is closely related to the idea of calibration [Barocas et al., 2023]. Thus, we make a mild assumption that the group sufficiency ratio $\omega_{\text{DP}}(y)$ can be calibrated by 1, i.e., $\mathbb{P}(Y = y \mid S = k, \hat{Y} = y) = \mathbb{P}(Y = y \mid S = k', \hat{Y} = y) = R$, where R is a calibration score. When two demographic groups are balanced, i.e., $\omega_{\text{DP}}(y) = 1$, we can see that the last inequality indicates the DP-based fairness disparity for binary classification problems. Therefore, we can also claim that the fairness metric DP can also be encouraged when reducing the risk disparity. \square

C Detailed Analysis of the Fair Influential Sampling Algorithm

C.1 Evaluating First-Order Influence Estimations Against Real Influence

Recall that the influence score derived in this paper primarily utilizes a first-order approach. Here, we will demonstrate how accurate the first-order estimation of the influence is in comparison to the real influence.

C.2 Comparative Analysis of Computational Costs

Recall that the proposed algorithm FIS needs to pre-calculate the accuracy loss and fairness loss for evaluating the performance of a certain example. However, the extra computation cost is comparable to the cost of traditional model training. Note that the main extra computation cost in FIS (Algorithm 1) mainly results from model gradients. Let p denote the number of model parameters, then the cost for computing the gradients is $O(p)$ per sample. Specifically, in each round that involves sampling, we need to calculate three parts of gradients: the gradients of $|U|$ unlabeled instances,

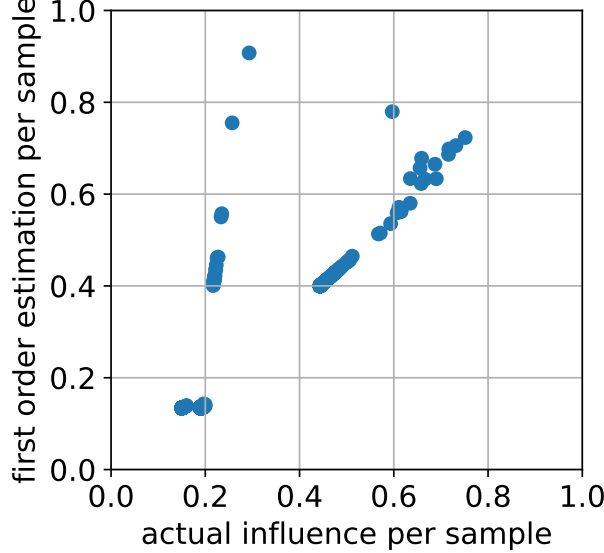


Figure 3: We validate how accurate the first-order estimation of the influence is in comparison to the real influence. The x -axis represents the actual influence per sample, and the y -axis represents the estimated influence. We observe that while some of the examples are away from the diagonal line (which indicates the estimation is inaccurate), the estimated influences for most of the data samples are very close to their actual influence values.

the average gradient of $|Q_v|$ validation instances w.r.t. accuracy loss, and the gradient of $|Q_v|$ validation instances w.r.t. fairness loss. Note that in general, $|Q_v| \ll |U|$. In practical implementation, to speed up the calculation of gradients over $|U|$ instances, we randomly sample 0.2-0.5% of the unlabeled dataset in each sampling batch. Additionally, we can increase the number of newly selected examples for each round (r) to save computation costs. In our experiments, we usually have 10-20 sampling rounds. For instance, running one experiment for the CelebA dataset on a single GPU roughly requires about 4 hours.

C.3 Exploration of the Labeling Strategies

Note that we provide a strategy that employs lowest-influence labels for annotating labels. This section will explore an alternative strategy that employs model predictions for the purpose of labeling. For completeness, we outline the two proposed labeling strategies as follows.

Strategy I **Use low-influence labels.** That is, $\hat{y} = \arg \min_{k \in [K]} |\text{Infl}_{\text{acc}}(x', k)|$, which corresponds to using the most uncertain point.

Strategy II **Rely on model prediction.** That is, $\hat{y} = \arg \max_{k \in [K]} f(x; \mathbf{w})[k]$, where $f(x; \mathbf{w})[y]$ indicates the model's prediction probability on label y .

Remark C.1. Suppose that the model is trained with cross-entropy loss. The labels obtained through **Strategy II** are sufficient to minimize the influence of the prediction component, i.e., $\text{Infl}_{\text{acc}}(x', k)$. That said, the **Strategy II** will produce similar labels as **Strategy I**.

Proof. Based on the definition of the influence of the prediction component, as delineated in Eq. (2), it becomes evident that the most uncertain points are obtained when the proxy labels closely align with the true labels. Consequently, the model predictions used in Strategy II also approximate the true labels to minimize the cross-entropy loss. Thus, in a certain sense, Strategy I and Strategy II can be considered equivalent. \square

D Omitted Proofs

In this section, we present complete proofs for the lemmas and theorems in Section 4 and 5, respectively.

D.1 Proof of Lemma 4.1

Lemma 4.1. *The influence of predictions on the validation dataset Q_v can be denoted by*

$$\text{Infl}_{\text{acc}}(z') := \sum_{n \in |Q_v|} \text{Infl}_{\text{acc}}(z', z_n^\circ) \approx -\eta \left\langle \partial_{\mathbf{w}_t} \ell(\mathbf{w}_t, z'), \sum_{n \in |Q_v|} \partial_{\mathbf{w}_t} \ell(\mathbf{w}, z_n^\circ) \right\rangle$$

Proof. Taking the first-order Taylor expansion, we will have

$$\ell(\mathbf{w}_{t+1}, z_n^\circ) \approx \ell(\mathbf{w}_t, z_n^\circ) + \left\langle \frac{\partial \ell(\mathbf{w}, z_n^\circ)}{\partial f(\mathbf{w}, x_n^\circ)} \Big|_{\mathbf{w}=\mathbf{w}_t}, f(\mathbf{w}_{t+1}, x_n^\circ) - f(\mathbf{w}_t, x_n^\circ) \right\rangle.$$

where we take this expansion with respect to $f(\mathbf{w}, x_n^\circ)$. Similarly, we have

$$\begin{aligned} f(\mathbf{w}_{t+1}, x_n^\circ) - f(\mathbf{w}_t, x_n^\circ) &\approx \left\langle \frac{\partial f(\mathbf{w}, x_n^\circ)}{\partial \mathbf{w}}, \mathbf{w}_{t+1} - \mathbf{w}_t \right\rangle \Big|_{\mathbf{w}=\mathbf{w}_t} \\ &= -\eta \left\langle \frac{\partial f(\mathbf{w}, x_n^\circ)}{\partial \mathbf{w}}, \frac{\partial \ell(\mathbf{w}, z')}{\partial \mathbf{w}} \right\rangle \Big|_{\mathbf{w}=\mathbf{w}_t}. \end{aligned}$$

where the last equality holds due to Eq. (1). Therefore,

$$\begin{aligned} \ell(\mathbf{w}_{t+1}, z_n^\circ) - \ell(\mathbf{w}_t, z_n^\circ) &\approx -\eta \left\langle \frac{\partial \ell(\mathbf{w}, z_n^\circ)}{\partial f(\mathbf{w}, x_n^\circ)}, \left\langle \frac{\partial f(\mathbf{w}, x_n^\circ)}{\partial \mathbf{w}}, \frac{\partial \ell(\mathbf{w}, z')}{\partial \mathbf{w}} \right\rangle \right\rangle \Big|_{\mathbf{w}=\mathbf{w}_t} \\ &= -\eta \left\langle \frac{\partial f(\mathbf{w}, x_n^\circ)}{\partial \mathbf{w}}, \frac{\partial \ell(\mathbf{w}, z')}{\partial \mathbf{w}} \right\rangle \Big|_{\mathbf{w}=\mathbf{w}_t}. \end{aligned}$$

Then the accuracy influence on the validation dataset V can be denoted by

$$\text{Infl}_{\text{acc}}(z') := \sum_{n \in |Q_v|} \text{Infl}_{\text{acc}}(z', z_n^\circ) \approx -\eta \left\langle \partial_{\mathbf{w}_t} \ell(\mathbf{w}_t, z'), \sum_{n \in |Q_v|} \partial_{\mathbf{w}_t} \ell(\mathbf{w}, z_n^\circ) \right\rangle$$

□

D.2 Proof of Lemma 4.2

Lemma 4.2. *The influence of fairness on the validation dataset Q_v can be denoted by*

$$\text{Infl}_{\text{fair}}(z') := \sum_{n \in |Q_v|} \text{Infl}_{\text{fair}}(z', z_n^\circ) \approx -\eta \sum_{n \in |Q_v|} \langle \partial_{\mathbf{w}_t} \ell(\mathbf{w}_t, z'), \partial_{\mathbf{w}_t} \phi(\mathbf{w}_t, z_n^\circ) \rangle$$

Proof. By first-order approximation, we have

$$\phi(\mathbf{w}_{t+1}, z_n^\circ) \approx \phi(\mathbf{w}_t, z_n^\circ) + \left\langle \frac{\partial \phi(\mathbf{w}_t, z_n^\circ)}{\partial f(\mathbf{w}, x_n^\circ)} \Big|_{\mathbf{w}=\mathbf{w}_t}, f(\mathbf{w}_{t+1}, x_n^\circ) - f(\mathbf{w}_t, x_n^\circ) \right\rangle.$$

Recall by first-order approximation, we have

$$f(\mathbf{w}_{t+1}, x_n^\circ) - f(\mathbf{w}_t, x_n^\circ) \approx -\eta \left\langle \frac{\partial f(\mathbf{w}, x_n^\circ)}{\partial \mathbf{w}}, \frac{\partial \ell(\mathbf{w}, z')}{\partial \mathbf{w}} \right\rangle \Big|_{\mathbf{w}=\mathbf{w}_t}.$$

Therefore,

$$\phi(\mathbf{w}_{t+1}, z_n^\circ) - \phi(\mathbf{w}_t, z_n^\circ) \approx -\eta \left\langle \frac{\partial \ell(\mathbf{w}, z')}{\partial \mathbf{w}}, \frac{\partial \phi(\mathbf{w}_t, z_n^\circ)}{\partial \mathbf{w}} \right\rangle \Big|_{\mathbf{w}=\mathbf{w}_t}$$

Note the loss function in the above equation should be ℓ since the model is updated with ℓ -loss. Therefore,

$$\text{Infl}_{\text{fair}}(z') = \sum_{n \in |Q_v|} \text{Infl}_{\text{fair}}(z', z_n^\circ) \approx -\eta \sum_{n \in |Q_v|} \left\langle \frac{\partial \ell(\mathbf{w}, z')}{\partial \mathbf{w}}, \frac{\partial \phi(\mathbf{w}_t, z_n^\circ)}{\partial \mathbf{w}} \right\rangle \Big|_{\mathbf{w}=\mathbf{w}_t}.$$

□

D.3 Proof of Theorem 5.1

Theorem 5.1. (Generalization error bound). Let $\text{dist}(\mathcal{P}, \mathcal{Q})$, G_P be defined therein. With probability at least $1 - \delta$ with $\delta \in (0, 1)$, the generalization error bound of the model trained on dataset P is

$$\mathcal{R}_{\mathcal{Q}}(\mathbf{w}^P) \leq \underbrace{G_P \cdot \text{dist}(\mathcal{P}, \mathcal{Q})}_{\text{distribution shift}} + \sqrt{\frac{\log(4/\delta)}{2|P|}} + \mathcal{R}_P(\mathbf{w}^P). \quad (9)$$

Note that the generalization error bound is predominantly influenced by the shift in distribution when we think of an overfitting model, i.e., the empirical risk $\mathcal{R}_P(\mathbf{w}^P) \rightarrow 0$. The detailed proof is presented as follows.

Proof. The generalization error bound is

$$\begin{aligned} \mathcal{R}_{\mathcal{Q}}(\mathbf{w}^P) &= \underbrace{\left(\mathcal{R}_{\mathcal{Q}}(\mathbf{w}^P) - \mathcal{R}_P(\mathbf{w}^P) \right)}_{\text{distribution shift}} + \underbrace{\left(\mathcal{R}_P(\mathbf{w}^P) - \mathcal{R}_P(\mathbf{w}^P) \right)}_{\text{Hoeffding's inequality}} + \underbrace{\mathcal{R}_P(\mathbf{w}^P)}_{\text{empirical risk}} \\ &\leq G_P \cdot \text{dist}(\mathcal{P}, \mathcal{Q}) + \sqrt{\frac{\log(4/\delta)}{2|P|}} + \mathcal{R}_P(\mathbf{w}^P) \end{aligned}$$

For the first term (distribution shift), we have

$$\begin{aligned} \mathcal{R}_{\mathcal{Q}}(\mathbf{w}^P) - \mathcal{R}_P(\mathbf{w}^P) &= \mathbb{E}_{z \sim \mathcal{Q}}[\ell(\mathbf{w}^P, z)] - \mathbb{E}_{z \sim \mathcal{P}}[\ell(\mathbf{w}^P, z)] \\ &= \sum_{i=1}^I p^{(\mathcal{Q})}(\pi = i) \mathbb{E}_{z \sim \pi_i}[\ell(\mathbf{w}^P, z)] - \sum_{i=1}^I p^{(\mathcal{P})}(\pi = i) \mathbb{E}_{z \sim \pi_i}[\ell(\mathbf{w}^P, z)] \\ &= \sum_{i=1}^I |p^{(\mathcal{P})}(\pi = i) - p^{(\mathcal{Q})}(\pi = i)| \mathbb{E}_{z \sim \pi_i}[\ell(\mathbf{w}^P, z)] \\ &\leq G_P \cdot \text{dist}(\mathcal{P}, \mathcal{Q}). \end{aligned}$$

where we define $\text{dist}(\mathcal{P}, \mathcal{Q}) = \sum_{i=1}^I |p^{(\mathcal{P})}(\pi = i) - p^{(\mathcal{Q})}(\pi = i)|$ and $\mathbb{E}_{z \sim \pi_i}[\ell(\mathbf{w}^P, z)] \leq G_P, \forall i \in I$ because of Assumption 5.2. To avoid misunderstanding, we use a subscript P of the constant G to clarify the corresponding model \mathbf{w}^P . Then, for the second term (Hoeffding inequality), with probability at least $1 - \delta$, we have $|\mathcal{R}_P(\mathbf{w}^P) - \mathcal{R}_P(\mathbf{w}^P)| \leq \sqrt{\frac{\log(4/\delta)}{2|P|}}$. \square

D.4 Proof of Theorem 5.2

Theorem 5.2. (Upper bound of fairness disparity). Suppose $\mathcal{R}_{\mathcal{Q}}(\cdot)$ follows Assumption 5.1. Let $\text{dist}(\mathcal{P}, \mathcal{Q})$, G_P , $\text{dist}(\mathcal{P}_k, \mathcal{Q}_k)$ and $\text{dist}(\mathcal{P}_k, P)$ be defined therein. Given model \mathbf{w}^P and \mathbf{w}^k trained exclusively on group k 's data P_k , with probability at least $1 - \delta$ with $\delta \in (0, 1)$, then the upper bound of the fairness disparity is

$$\mathcal{R}_{\mathcal{Q}_k}(\mathbf{w}^P) - \mathcal{R}_{\mathcal{Q}}(\mathbf{w}^P) \leq \underbrace{G_P \cdot \text{dist}(\mathcal{P}, \mathcal{Q})}_{\text{distribution shift}} + \underbrace{4L^2 G^2 \cdot \text{dist}(P_k, P)^2}_{\text{group gap}} + G_k \cdot \text{dist}(\mathcal{P}_k, \mathcal{Q}_k) + \Upsilon.$$

where

$$\Upsilon = \sqrt{\frac{\log(4/\delta)}{2|P|}} + \sqrt{\frac{\log(4/\delta)}{2|P_k|}} + \varpi + \varpi_k$$

Note that $\mathbb{E}_{z \sim \pi_i}[\ell(\mathbf{w}^k, z)] \leq G_k$, $\varpi = \mathcal{R}_P(\mathbf{w}^P) - \mathcal{R}_{\mathcal{Q}}^*(\mathbf{w}^Q)$ and $\varpi_k = \mathcal{R}_{P_k}(\mathbf{w}^k) - \mathcal{R}_{\mathcal{Q}_k}^*(\mathbf{w}^{\mathcal{Q}_k})$. Specifically, ϖ and ϖ_k can be regarded as constants because $\mathcal{R}_P(\mathbf{w}^P)$ and $\mathcal{R}_{P_k}(\mathbf{w}^k)$ correspond to the empirical risks, $\mathcal{R}_{\mathcal{Q}}^*(\mathbf{w}^Q)$ and $\mathcal{R}_{\mathcal{Q}_k}^*(\mathbf{w}^{\mathcal{Q}_k})$ represent the ideal minimal empirical risk of model \mathbf{w}^Q trained on distribution \mathcal{Q} and \mathcal{Q}_k , respectively. Moreover, these quantities ϖ and ϖ_k are not taken into account during the training phase, but rather in relation to the final model.

Proof. First of all, we have

$$\begin{aligned}
& \mathcal{R}_{\mathcal{Q}_k}(\mathbf{w}^P) - \mathcal{R}_{\mathcal{Q}}(\mathbf{w}^P) \\
&= (\mathcal{R}_{\mathcal{Q}}(\mathbf{w}^{P_k}) - \mathcal{R}_{\mathcal{Q}}(\mathbf{w}^P)) + (\mathcal{R}_{\mathcal{Q}_k}(\mathbf{w}^P) - \mathcal{R}_{\mathcal{Q}}(\mathbf{w}^{P_k})) \\
&= (\mathcal{R}_{\mathcal{Q}}(\mathbf{w}^{P_k}) - \mathcal{R}_{\mathcal{Q}}(\mathbf{w}^P)) + (\mathcal{R}_{\mathcal{Q}_k}(\mathbf{w}^P) - \mathcal{R}_{\mathcal{Q}_k}(\mathbf{w}^{P_k})) + (\mathcal{R}_{\mathcal{Q}_k}(\mathbf{w}^{P_k}) - \mathcal{R}_{\mathcal{Q}}(\mathbf{w}^{P_k})) \\
&\leq (\mathcal{R}_{\mathcal{Q}}(\mathbf{w}^{P_k}) - \mathcal{R}_{\mathcal{Q}}(\mathbf{w}^P)) + (\mathcal{R}_{\mathcal{Q}_k}(\mathbf{w}^P) - \mathcal{R}_{\mathcal{Q}_k}(\mathbf{w}^{P_k}))
\end{aligned}$$

where \mathbf{w}^{P_k} represents the model trained exclusively on group k 's data. For simplicity, when there is no confusion, we use \mathbf{w}^k to substitute \mathbf{w}^{P_k} . The inequality $\mathcal{R}_{\mathcal{Q}_k}(\mathbf{w}^k) - \mathcal{R}_{\mathcal{Q}}(\mathbf{w}^k) \leq 0$ holds due to the fact that the model tailored for a single group k can not generalize well to the entirety of the test set \mathcal{Q} .

Then, for the first term, we have

$$\begin{aligned}
\mathcal{R}_{\mathcal{Q}}(\mathbf{w}^k) - \mathcal{R}_{\mathcal{Q}}(\mathbf{w}^P) &\stackrel{(a)}{\leq} \langle \nabla \mathcal{R}_{\mathcal{Q}}(\mathbf{w}^P), \mathbf{w}^k - \mathbf{w}^P \rangle + \frac{L}{2} \|\mathbf{w}^k - \mathbf{w}^P\|^2 \\
&\stackrel{(b)}{\leq} L \|\mathbf{w}^k - \mathbf{w}^P\|^2 + \frac{1}{2L} \|\nabla \mathcal{R}_{\mathcal{Q}}(\mathbf{w}^P)\|^2 \\
&\stackrel{(c)}{\leq} \underbrace{L \|\mathbf{w}^k - \mathbf{w}^P\|^2}_{\text{group gap}} + \underbrace{(\mathcal{R}_{\mathcal{Q}}(\mathbf{w}^P) - \mathcal{R}_{\mathcal{Q}}^*(\mathbf{w}^{\mathcal{Q}}))}_{\text{train-test model gap}}
\end{aligned}$$

where inequality (a) holds because of the L-smoothness of expected loss $\mathcal{R}_{\mathcal{Q}}(\cdot)$, i.e., Assumption 5.1. Specifically, inequality (b) holds because, by Cauchy-Schwarz inequality and AM-GM inequality, we have

$$\langle \nabla \mathcal{R}_{\mathcal{Q}}(\mathbf{w}^P), \mathbf{w}^k - \mathbf{w}^P \rangle \leq \frac{L}{2} \|\mathbf{w}^k - \mathbf{w}^P\|^2 + \frac{1}{2L} \|\nabla \mathcal{R}_{\mathcal{Q}}(\mathbf{w}^P)\|^2.$$

Then, inequality (c) holds due to the L-smoothness of $\mathcal{R}_{\mathcal{Q}}(\cdot)$ (Assumption 5.1), we can get a variant of Polak-Łojasiewicz inequality, which follows

$$\|\nabla \mathcal{R}_{\mathcal{Q}}(\mathbf{w}^P)\|^2 \leq 2L(\mathcal{R}_{\mathcal{Q}}(\mathbf{w}^P) - \mathcal{R}_{\mathcal{Q}}^*(\mathbf{w}^{\mathcal{Q}})).$$

Following a similar idea, for the second term, we also have

$$\mathcal{R}_{\mathcal{Q}_k}(\mathbf{w}^P) - \mathcal{R}_{\mathcal{Q}_k}(\mathbf{w}^k) \leq L \|\mathbf{w}^P - \mathbf{w}^k\|^2 + (\mathcal{R}_{\mathcal{Q}_k}(\mathbf{w}^k) - \mathcal{R}_{\mathcal{Q}_k}^*(\mathbf{w}^{\mathcal{Q}_k}))$$

Combined with two terms, we have

$$\mathcal{R}_{\mathcal{Q}_k}(\mathbf{w}^P) - \mathcal{R}_{\mathcal{Q}}(\mathbf{w}^P) \leq \underbrace{(\mathcal{R}_{\mathcal{Q}}(\mathbf{w}^P) - \mathcal{R}_{\mathcal{Q}}^*(\mathbf{w}^{\mathcal{Q}}))}_{\text{train-test model gap}} + \underbrace{2L \|\mathbf{w}^k - \mathbf{w}^P\|^2}_{\text{group gap}} + (\mathcal{R}_{\mathcal{Q}_k}(\mathbf{w}^k) - \mathcal{R}_{\mathcal{Q}_k}^*(\mathbf{w}^{\mathcal{Q}_k}))$$

Lastly, integrating with Lemma D.1, D.2 and D.3, we can finish the proof. □

Lemma D.1. *(Train-test model gap) With probability at least $1 - \delta$, given the model \mathbf{w}^P trained on train set P , we have*

$$\mathcal{R}_{\mathcal{Q}}(\mathbf{w}^P) - \mathcal{R}_{\mathcal{Q}}^*(\mathbf{w}^{\mathcal{Q}}) \leq G_P \cdot \text{dist}(\mathcal{P}, \mathcal{Q}) + \sqrt{\frac{\log(4/\delta)}{2|P|}} + \varpi.$$

where $\text{dist}(\mathcal{P}, \mathcal{Q}) = \sum_{i=1}^I |p^{(\mathcal{P})}(\pi = i) - p^{(\mathcal{Q})}(\pi = i)|$ and $\mathbb{E}_{z \sim \pi_i} [\ell(\mathbf{w}^P, z)] \leq G_P, \forall i \in I$, and a constant $\varpi := \mathcal{R}_P(\mathbf{w}^P) - \mathcal{R}_{\mathcal{Q}}^*(\mathbf{w}^{\mathcal{Q}})$.

Proof. First of all, we have,

$$\begin{aligned}
\mathcal{R}_{\mathcal{Q}}(\mathbf{w}^P) - \mathcal{R}_{\mathcal{Q}}^*(\mathbf{w}^{\mathcal{Q}}) &= \left(\mathcal{R}_{\mathcal{Q}}(\mathbf{w}^P) - \mathcal{R}_{\mathcal{P}}(\mathbf{w}^P) \right) + \mathcal{R}_{\mathcal{P}}(\mathbf{w}^P) - \mathcal{R}_{\mathcal{Q}}^*(\mathbf{w}^{\mathcal{Q}}) \\
&\leq G \cdot \text{dist}(\mathcal{P}, \mathcal{Q}) + \mathcal{R}_{\mathcal{P}}(\mathbf{w}^P) - \mathcal{R}_{\mathcal{Q}}^*(\mathbf{w}^{\mathcal{Q}}) \\
&\leq \underbrace{G \cdot \text{dist}(\mathcal{P}, \mathcal{Q})}_{\text{distribution shift}} + \underbrace{\left(\mathcal{R}_{\mathcal{P}}(\mathbf{w}^P) - \mathcal{R}_{\mathcal{P}}(\mathbf{w}^P) \right)}_{\text{Hoeffding's inequality}} + \underbrace{\left(\mathcal{R}_{\mathcal{P}}(\mathbf{w}^P) - \mathcal{R}_{\mathcal{Q}}^*(\mathbf{w}^{\mathcal{Q}}) \right)}_{\text{overfitting \& ideal case}}
\end{aligned}$$

For the first term (distribution shift), we have

$$\begin{aligned}
\mathcal{R}_{\mathcal{Q}}(\mathbf{w}^P) - \mathcal{R}_{\mathcal{P}}(\mathbf{w}^P) &= \mathbb{E}_{z \sim \mathcal{Q}}[\ell(\mathbf{w}^P, z)] - \mathbb{E}_{z \sim \mathcal{P}}[\ell(\mathbf{w}^P, z)] \\
&= \sum_{i=1}^I p^{(\mathcal{Q})}(\pi = i) \mathbb{E}_{z \sim \pi_i}[\ell(\mathbf{w}^P, z)] - \sum_{i=1}^I p^{(\mathcal{P})}(\pi = i) \mathbb{E}_{z \sim \pi_i}[\ell(\mathbf{w}^P, z)] \\
&\leq \sum_{i=1}^I |p^{(\mathcal{P})}(\pi = i) - p^{(\mathcal{Q})}(\pi = i)| \mathbb{E}_{z \sim \pi_i}[\ell(\mathbf{w}^P, z)] \\
&\leq G_P \cdot \text{dist}(\mathcal{P}, \mathcal{Q}).
\end{aligned}$$

where we define $\text{dist}(\mathcal{P}, \mathcal{Q}) = \sum_{i=1}^I |p^{(\mathcal{P})}(\pi = i) - p^{(\mathcal{Q})}(\pi = i)|$ and $\mathbb{E}_{z \sim \pi_i}[\ell(\mathbf{w}^P, z)] \leq G_P, \forall i \in I$ because of Assumption 5.2. For the second term, with probability at least $1 - \delta$, we have $|\mathcal{R}_{\mathcal{P}}(\mathbf{w}^P) - \mathcal{R}_P(\mathbf{w}^P)| \leq \sqrt{\frac{\log(4/\delta)}{2|P|}}$. Note that the third term $\mathcal{R}_P(\mathbf{w}^P) - \mathcal{R}_{\mathcal{Q}}^*(\mathbf{w}^{\mathcal{Q}})$ can be regarded as a constant ϖ because $\mathcal{R}_P(\mathbf{w}^P)$ is the empirical risk and $\mathcal{R}_{\mathcal{Q}}^*(\mathbf{w}^{\mathcal{Q}})$ is the ideal minimal empirical risk of model $\mathbf{w}^{\mathcal{Q}}$ trained on distribution \mathcal{Q} .

Therefore, with probability at least $1 - \delta$, given model \mathbf{w}^P ,

$$\mathcal{R}_{\mathcal{Q}}(\mathbf{w}^P) - \mathcal{R}_{\mathcal{Q}}^*(\mathbf{w}^{\mathcal{Q}}) \leq G_P \cdot \text{dist}(\mathcal{P}, \mathcal{Q}) + \sqrt{\frac{\log(4/\delta)}{2|P|}} + \varpi.$$

□

Lemma D.2. (Group gap) Suppose Assumptions 5.1 and 5.2 hold for empirical risk $\mathcal{R}_P(\cdot)$, then we have

$$\|\mathbf{w}^k - \mathbf{w}^P\|^2 \leq 2LG^2 \left(\sum_{i=1}^I \left| p^{(k)}(\pi = i) - p^{(P)}(\pi = i) \right| \right)^2.$$

Proof. According to the above definition, we similarly define the following empirical risk $\mathcal{R}_{P_k}(\mathbf{w})$ over group k 's data P_k by splitting samples according to their marginal distributions, shown as follows.

$$\mathcal{R}_{P_k}(\mathbf{w}) := \sum_{i=1}^I p^{(k)}(\pi = i) \mathbb{E}_{z \sim \pi_i}[\ell(\mathbf{w}, z)].$$

Let η_t indicate the learning rate of epoch t . Then, for each epoch t , group k 's optimizer performs SGD as follows:

$$\mathbf{w}_t^k = \mathbf{w}_{t-1}^k - \eta_t \sum_{i=1}^I p^{(k)}(\pi = i) \nabla_{\mathbf{w}} \mathbb{E}_{z \sim \pi_i}[\ell(\mathbf{w}_{t-1}^k, z)].$$

For any epoch $t + 1$, we have

$$\begin{aligned}
& \|\mathbf{w}_{t+1}^k - \mathbf{w}_{t+1}^P\|^2 \\
&= \|\mathbf{w}_t^k - \eta_t \sum_{i=1}^I p^{(k)}(\pi = i) \nabla_{\mathbf{w}} \mathbb{E}_{z \sim \pi_i} [\ell(\mathbf{w}_t^k, z)] - \mathbf{w}_t^P + \eta_t \sum_{i=1}^I p^{(P)}(\pi = i) \nabla_{\mathbf{w}} \mathbb{E}_{z \sim \pi_i} [\ell(\mathbf{w}_t^P, z)]\|^2 \\
&\leq \|\mathbf{w}_t^k - \mathbf{w}_t^P\|^2 + \eta_t^2 \left\| \sum_{i=1}^I p^{(k)}(\pi = i) \nabla_{\mathbf{w}} \mathbb{E}_{z \sim \pi_i} [\ell(\mathbf{w}_t^k, z)] - \sum_{i=1}^I p^{(P)}(\pi = i) \nabla_{\mathbf{w}} \mathbb{E}_{z \sim \pi_i} [\ell(\mathbf{w}_t^P, z)] \right\|^2 \\
&\leq \|\mathbf{w}_t^k - \mathbf{w}_t^P\|^2 + 2\eta_t^2 \left\| \sum_{i=1}^I p^{(P)}(\pi = i) L_{\pi_i} \left[\nabla_{\mathbf{w}} \mathbb{E}_{z \sim \pi_i} [\ell(\mathbf{w}_t^k, z)] - \nabla_{\mathbf{w}} \mathbb{E}_{z \sim \pi_i} [\ell(\mathbf{w}_t^P, z)] \right] \right\|^2 \\
&\quad + 2\eta_t^2 \left\| \sum_{i=1}^I \left(p^{(k)}(\pi = i) - p^{(P)}(\pi = i) \right) \nabla_{\mathbf{w}} \mathbb{E}_{z \sim \pi_i} [\ell(\mathbf{w}_t^P, z)] \right\|^2 \\
&\leq \|\mathbf{w}_t^k - \mathbf{w}_t^P\|^2 + 2\eta_t^2 \left(\sum_{i=1}^I p^{(k)}(\pi = i) L_{\pi_i} \right)^2 \|\mathbf{w}_t^k - \mathbf{w}_t^P\|^2 \\
&\quad + 2L\eta_t^2 g_{\max}^2(\mathbf{w}_t^Q) \left(\sum_{i=1}^I |p^{(k)}(\pi = i) - p^{(P)}(\pi = i)| \right)^2 \\
&\leq \left(1 + 2\eta_t^2 \left(\sum_{i=1}^I p^{(k)}(\pi = i) L_{\pi_i} \right)^2 \right) \|\mathbf{w}_t^k - \mathbf{w}_t^P\|^2 \\
&\quad + 2L\eta_t^2 g_{\max}^2(\mathbf{w}_t^Q) \left(\sum_{i=1}^I |p^{(k)}(\pi = i) - p^{(P)}(\pi = i)| \right)^2 \\
&\leq (1 + 2\eta_t^2 L^2) \|\mathbf{w}_t^k - \mathbf{w}_t^P\|^2 + 2L\eta_t^2 G^2 \left(\sum_{i=1}^I |p^{(k)}(\pi = i) - p^{(P)}(\pi = i)| \right)^2.
\end{aligned}$$

where the third inequality holds since we assume that $\nabla_{\mathbf{w}} \mathbb{E}_{z \sim \pi_i} [\ell(\mathbf{w}, z)]$ is L_{π_i} -Lipschitz continuous, i.e., $\|\nabla_{\mathbf{w}} \mathbb{E}_{z \sim \pi_i} [\ell(\mathbf{w}_t^k, z)] - \nabla_{\mathbf{w}} \mathbb{E}_{z \sim \pi_i} [\ell(\mathbf{w}_t^P, z)]\| \leq L_{\pi_i} \|\mathbf{w}_t^k - \mathbf{w}_t^P\|$, and denote $g_{\max}(\mathbf{w}_t^P) = \max_{i=1}^I \|\nabla_{\mathbf{w}} \mathbb{E}_{z \sim \pi_i} [\ell(\mathbf{w}_t^P, z)]\|$. The last inequality holds because the above-mentioned assumption that $L = L_{\pi_i} = L_{\pi}, \forall i \in I$, i.e., Lipschitz-continuity will not be affected by the samples' classes. Then, $g_{\max}(\mathbf{w}_t^P) \leq G$ because of Assumption 5.2.

For T training epochs, we have

$$\begin{aligned}
& \|\mathbf{w}_T^k - \mathbf{w}_T^P\|^2 \\
&\leq (1 + 2\eta_t^2 L^2) \|\mathbf{w}_{T-1}^k - \mathbf{w}_{T-1}^P\|^2 + 2L\eta_t^2 G^2 \left(\sum_{i=1}^I |p^{(k)}(\pi = i) - p^{(P)}(\pi = i)| \right)^2 \\
&\leq \prod_{t=0}^T (1 + 2\eta_t^2 L^2)^t \|\mathbf{w}_0^k - \mathbf{w}_0^P\|^2 + 2LG^2 \sum_{t=0}^T (\eta_t^2 (1 + 2\eta_t^2 L^2))^t \left(\sum_{i=1}^I |p^{(k)}(\pi = i) - p^{(P)}(\pi = i)| \right)^2 \\
&\leq 2LG^2 \sum_{t=0}^T (\eta_t^2 (1 + 2\eta_t^2 L^2))^t \left(\sum_{i=1}^I |p^{(k)}(\pi = i) - p^{(P)}(\pi = i)| \right)^2.
\end{aligned}$$

where the last inequality holds because the initial models are the same, i.e., $\mathbf{w}_0 = \mathbf{w}_0^k = \mathbf{w}_0^P, \forall k$. When the condition $\eta_t^2 < \frac{1}{\sqrt{2}L}$ satisfies, $2LG^2 \sum_{t=0}^T (\eta_t^2 (1 + 2\eta_t^2 L^2))^t$ can be simplified as $2LG^2$, which is independent of the learning algorithm. This condition is easy to be satisfied since the learning rate η_t is a small value (< 0.0001). \square

Lemma D.3. *With probability at least $1 - \delta$, given the model \mathbf{w}^k trained on group k 's dataset P_k , we have*

$$\mathcal{R}_{\mathcal{Q}_k}(\mathbf{w}^k) - \mathcal{R}_{\mathcal{Q}_k}^*(\mathbf{w}^{\mathcal{Q}_k}) \leq G_k \cdot \text{dist}(\mathcal{P}_k, \mathcal{Q}_k) + \sqrt{\frac{\log(4/\delta)}{2|P_k|}} + \varpi_k.$$

where $\text{dist}(\mathcal{P}_k, \mathcal{Q}_k) = \sum_{i=1}^I |p^{(\mathcal{P}_k)}(\pi = i) - p^{(\mathcal{Q}_k)}(\pi = i)|$ and $\mathbb{E}_{z \sim \pi_i}[\ell(\mathbf{w}^k, z)] \leq G_k, \forall i \in I$, and $\varpi_k := \mathcal{R}_{\mathcal{P}_k}(\mathbf{w}^k) - \mathcal{R}_{\mathcal{Q}_k}^*(\mathbf{w}^{\mathcal{Q}_k})$.

Proof. Building upon the proof idea presented in Lemma D.1, for completeness, we provide a full proof here. Firstly, we have,

$$\begin{aligned} & \mathcal{R}_{\mathcal{Q}_k}(\mathbf{w}^k) - \mathcal{R}_{\mathcal{Q}_k}^*(\mathbf{w}^{\mathcal{Q}_k}) \\ &= \underbrace{(\mathcal{R}_{\mathcal{Q}_k}(\mathbf{w}^k) - \mathcal{R}_{\mathcal{P}_k}(\mathbf{w}^k))}_{\text{distribution shift}} + \underbrace{(\mathcal{R}_{\mathcal{P}_k}(\mathbf{w}^k) - \mathcal{R}_{\mathcal{P}_k}(\mathbf{w}^k))}_{\text{Hoeffding's inequality}} + \underbrace{(\mathcal{R}_{\mathcal{P}_k}(\mathbf{w}^k) - \mathcal{R}_{\mathcal{Q}_k}^*(\mathbf{w}^{\mathcal{Q}_k}))}_{\text{overfitting \& ideal case}} \end{aligned}$$

For the first term, we have

$$\begin{aligned} \mathcal{R}_{\mathcal{Q}_k}(\mathbf{w}^k) - \mathcal{R}_{\mathcal{P}_k}(\mathbf{w}^k) &= \sum_{i=1}^I p^{(\mathcal{Q}_k)}(\pi = i) \mathbb{E}_{z \sim \pi_i}[\ell(\mathbf{w}^k, z)] - \sum_{i=1}^I p^{(\mathcal{P}_k)}(\pi = i) \mathbb{E}_{z \sim \pi_i}[\ell(\mathbf{w}^k, z)] \\ &\leq \sum_{i=1}^I |p^{(\mathcal{P}_k)}(\pi = i) - p^{(\mathcal{Q}_k)}(\pi = i)| \mathbb{E}_{z \sim \pi_i}[\ell(\mathbf{w}^k, z)] \\ &\leq G_k \cdot \text{dist}(\mathcal{P}_k, \mathcal{Q}_k). \end{aligned}$$

where $\text{dist}(\mathcal{P}_k, \mathcal{Q}_k) := \sum_{i=1}^I |p^{(\mathcal{P}_k)}(\pi = i) - p^{(\mathcal{Q}_k)}(\pi = i)|$ and $\mathbb{E}_{z \sim \pi_i}[\ell(\mathbf{w}^k, z)] \leq G_k, \forall i \in I$ due to Assumption 5.2. Recall that the constant G_k clarifies the bound of loss on the corresponding model \mathbf{w}^k . For the second term, with probability at least $1 - \delta$, we have $|\mathcal{R}_{\mathcal{P}_k}(\mathbf{w}^k) - \mathcal{R}_{\mathcal{P}_k}(\mathbf{w}^k)| \leq \sqrt{\frac{\log(4/\delta)}{2|P_k|}}$. For the third term, we define $\varpi_k := \mathcal{R}_{\mathcal{P}_k}(\mathbf{w}^k) - \mathcal{R}_{\mathcal{Q}_k}^*(\mathbf{w}^{\mathcal{Q}_k})$, which can be regarded as a constant. This is because $\mathcal{R}_{\mathcal{P}_k}(\mathbf{w}^k)$ represents empirical risk and $\mathcal{R}_{\mathcal{Q}_k}^*(\mathbf{w}^{\mathcal{Q}_k})$ is the ideal minimal empirical risk of model $\mathbf{w}^{\mathcal{Q}_k}$ trained on sub-distribution \mathcal{Q}_k .

Therefore, with probability at least $1 - \delta$, given model \mathbf{w}^k ,

$$\mathcal{R}_{\mathcal{Q}_k}(\mathbf{w}^k) - \mathcal{R}_{\mathcal{Q}_k}^*(\mathbf{w}^{\mathcal{Q}_k}) \leq G_k \cdot \text{dist}(\mathcal{P}_k, \mathcal{Q}_k) + \sqrt{\frac{\log(4/\delta)}{2|P_k|}} + \varpi_k.$$

□

E More Experimental Results

E.1 Datasets and Parameter Settings

We empirically evaluate FIS on the CelebA dataset, an image dataset commonly used in the fairness literature [Liu et al., 2015]. We also evaluate FIS on two tabular datasets: UCI Adult [Asuncion and Newman, 2007] and Compas Dataset [Angwin et al., 2016].

E.1.1 CelebA Dataset

Dataset details CelebA [Liu et al., 2015] is an image dataset with 202,599 celebrity face images annotated with 40 attributes, including gender, hair colour, age, smiling, etc. The sensitive attribute is gender: $S = \{\text{Men}, \text{Women}\}$. We select four binary classification targets, including smiling, attractive, young, and big nose. For example, the task is to predict whether a person in an image is young ($Y = 1$) or non-young ($Y = 0$), among other attribute predictions.

Hyper-parameter details In all our experiments using CelebA dataset, we train a vision transformer with patch size (8, 8) using SGD optimizer and a batch size of 128. The epochs are split into two phases: warm-up epochs (5 epochs) and training epochs (10 epochs). The default label budget per round, which represents the number of solicited data samples, is set to 256. Additionally, the default values for learning rate, momentum, and weight decay are 0.01, 0.9, and 0.0005, respectively. We initially allocate 2% of the training set for training purposes and the remaining 98% for sampling. Then, we randomly select 10% of the test data for validation. For JTT, we explore 10% data for training purposes with weights $\lambda = 20$ for retraining misclassified examples.

E.1.2 UCI Adult Dataset

Dataset details. The Adult dataset [Asuncion and Newman, 2007] predicts whether an individual’s annual income falls below or exceeds $50K$, denoted as $Y = 0$ and $Y = 1$, respectively. This prediction is based on a variety of continuous and categorical attributes, including education level, age, gender, occupation, etc. The default sensitive attribute in this dataset is gender $S = \{\text{Men, Women}\}$ [Zemel et al., 2013]. In particular, we also group this dataset using age $S = \{\text{Teenager, Non-teenager}\}$. To achieve a balanced age distribution in the dataset, individuals with an age of less than 30 are grouped as “Teenager”. The dataset contains a total of 45,000 instances. The dataset exhibits an imbalance: there are twice as many men as women, and only 15% of those with high incomes are women.

Hyper-parameter details. In the experiments using Adult dataset, we train a two-layer ReLU network with a hidden size of 64. The epochs are split into two phases: warm-up epochs (100 epochs) and training epochs (60 epochs). The default label budget per round, which represents the number of solicited data samples, is set to 1024. Additionally, the default values for learning rate, momentum, and weight decay are 0.00001, 0.9, and 0.0005, respectively. We resample the datasets to balance the class and group membership [Chawla et al., 2002]. The dataset is randomly split into a train and a test set in a ratio of 80 to 20. Then, we randomly re-select 20% of the training set for initial training and the remaining 80% for sampling. Also, 20% examples of the test set are selected to form a validation set. We utilize the whole model to compute the prediction influence and fairness for examples. Then, we randomly select 10% of the test data for validation. For JTT, we explore 30% data for training purposes with weights $\lambda = 20$ for retraining misclassified examples.

E.1.3 Compas Dataset

Dataset details. Compas dataset, also known as the Correctional Offender Management Profiling for Alternative Sanctions dataset, is a collection of data related to criminal defendants. It contains information on approximately 6,172 individuals who were assessed for risk of re-offending. The primary task associated with this dataset is predicting whether a defendant will re-offend ($Y = 1$) or not ($Y = 0$) within a certain time frame after their release. The sensitive attribute is often considered to be race, specifically whether the individual is classified as African American or not.

Hyper-parameter details. In the experiments using the Compas dataset, we train a multi-layer neural network with one hidden layer consisting of 64 neurons. The epochs are split into two phases: warm-up epochs (20 epochs) and training epochs (50 epochs). The default label budget per round, which represents the number of solicited data samples, is set to 128. Furthermore, the default values for learning rate, momentum, and weight decay are 0.01, 0.9, and 0.0005, respectively. We resample the datasets to balance the class and group membership [Chawla et al., 2002]. The dataset is initially split into training and test sets at an 80-20 ratio. Then, we further split 20% of the training set for initial training, reserving the remaining 80% for sampling. Additionally, 20% of the test set is selected to create a validation set. We use the entire model to calculate prediction influence and evaluate fairness for the dataset examples.

E.2 Full Version of Experimental Results

E.3 The Impact of Label Budgets

Exploring the impact of label budgets. In our study, we examine how varying label budgets r influence the balance between accuracy and fairness. We present the results of test accuracy and fairness disparity across different label budgets on the CelebA, Compas, and Adult datasets. In these experiments, we use the demographics parity (DP) as our fairness metric. For convenience, we maintain a fixed label budget per round, using rounds of label budget allocation to demonstrate its impact. The designated label budgets per round for the CelebA, Compas, and Adult are 256, 128, and 512, respectively. In the following figures, the x -axis is both the number of label budget rounds. The y -axis for the left and right sub-figures are test accuracy and DP gap, respectively. As observed in Figures 4-6, compared to the three baselines (BALD, JTT-20 and ISAL), our approach substantially reduces the DP gap without sacrificing test accuracy.

Specifically, on the Adult dataset, both accuracy and fairness violation converge to similar numerical values when the budget is lower than 20, suggesting a potential overfitting of the model to insufficient training examples. With a larger budget, our algorithms outperform other baseline methods, achieving higher accuracy and lower demographic disparity.

E.4 The Role of Validation Dataset Size

In this subsection, we explore the impact of adjusting the validation set size on our algorithm’s performance. We present the test accuracy and fairness disparity across different validation set sizes on the CelebA, Compas, and Adult datasets. Note that the default validation set size for image and tabular datasets is set to 1% and 4% of the whole dataset size,

Table 3: We report the (test_accuracy, fairnessViolation) for evaluating the performance on the **CelebA** dataset with two binary classification targets Young and Big Nose. We select gender as the sensitive attribute.

$\epsilon = 0.05$		CelebA - Young		
	DP	EOP	EOd	
Base(ERM)	(0.755 \pm 0.002, 0.190 \pm 0.017)	(0.759 \pm 0.005, 0.102 \pm 0.005)	(0.755 \pm 0.002, 0.182 \pm 0.018)	
Random	(0.763 \pm 0.008, 0.158 \pm 0.016)	(0.698 \pm 0.109, 0.075 \pm 0.021)	(0.766 \pm 0.011, 0.156 \pm 0.017)	
BALD	(0.776 \pm 0.021, 0.165 \pm 0.019)	(0.775 \pm 0.020, 0.076 \pm 0.007)	(0.779 \pm 0.005, 0.162 \pm 0.021)	
ISAL	(0.781 \pm 0.020, 0.180 \pm 0.014)	(0.781 \pm 0.020, 0.084 \pm 0.006)	(0.780 \pm 0.021, 0.173 \pm 0.012)	
JTT-20	(0.774 \pm 0.026, 0.167 \pm 0.016)	(0.774 \pm 0.024, 0.083 \pm 0.007)	(0.772 \pm 0.023, 0.171 \pm 0.025)	
FIS	(0.763 \pm 0.004, 0.104 \pm 0.059)	(0.773 \pm 0.003, 0.041 \pm 0.015)	(0.763 \pm 0.005, 0.118 \pm 0.074)	

$\epsilon = 0.05$		CelebA - Big Nose		
	DP	EOP	EOd	
Base(ERM)	(0.752 \pm 0.024, 0.198 \pm 0.034)	(0.755 \pm 0.022, 0.206 \pm 0.018)	(0.755 \pm 0.022, 0.183 \pm 0.029)	
Random	(0.760 \pm 0.009, 0.177 \pm 0.014)	(0.757 \pm 0.004, 0.190 \pm 0.029)	(0.759 \pm 0.006, 0.167 \pm 0.029)	
BALD	(0.777 \pm 0.004, 0.184 \pm 0.016)	(0.765 \pm 0.003, 0.209 \pm 0.014)	(0.770 \pm 0.004, 0.170 \pm 0.015)	
ISAL	(0.782 \pm 0.001, 0.148 \pm 0.059)	(0.782 \pm 0.001, 0.154 \pm 0.080)	(0.779 \pm 0.006, 0.145 \pm 0.065)	
JTT-20	(0.771 \pm 0.014, 0.191 \pm 0.036)	(0.758 \pm 0.026, 0.223 \pm 0.018)	(0.764 \pm 0.019, 0.193 \pm 0.016)	
FIS	(0.779 \pm 0.009, 0.089 \pm 0.076)	(0.780 \pm 0.013, 0.046 \pm 0.072)	(0.772 \pm 0.015, 0.062 \pm 0.081)	

Table 4: The performance results of (test_accuracy, fairnessViolation) on the **Adult** dataset. The sensitive attributes is age.

$\epsilon = 0.05$		Income (age)		
	DP	EOP	EOd	
Base(ERM)	(0.665 \pm 0.045, 0.255 \pm 0.041)	(0.665 \pm 0.045, 0.115 \pm 0.036)	(0.665 \pm 0.045, 0.158 \pm 0.030)	
Random	(0.765 \pm 0.021, 0.209 \pm 0.042)	(0.758 \pm 0.027, 0.127 \pm 0.013)	(0.764 \pm 0.018, 0.133 \pm 0.027)	
BALD	(0.767 \pm 0.019, 0.203 \pm 0.017)	(0.703 \pm 0.111, 0.117 \pm 0.013)	(0.763 \pm 0.022, 0.128 \pm 0.014)	
ISAL	(0.765 \pm 0.020, 0.215 \pm 0.011)	(0.755 \pm 0.028, 0.128 \pm 0.013)	(0.761 \pm 0.024, 0.138 \pm 0.009)	
JTT-20	(0.751 \pm 0.013, 0.262 \pm 0.020)	(0.742 \pm 0.018, 0.149 \pm 0.021)	(0.745 \pm 0.014, 0.171 \pm 0.012)	
FIS	(0.766 \pm 0.013, 0.214 \pm 0.009)	(0.757 \pm 0.034, 0.113 \pm 0.017)	(0.763 \pm 0.011, 0.143 \pm 0.023)	

Table 5: The performance results of (test_accuracy, fairnessViolation) on the **COMPAS** dataset. The selected sensitive attribute is race.

$\epsilon = 0.05$		recidivism		
	DP	EOP	EOd	
Base(ERM)	(0.675 \pm 0.005, 0.333 \pm 0.008)	(0.675 \pm 0.005, 0.267 \pm 0.010)	(0.675 \pm 0.005, 0.284 \pm 0.010)	
Random	(0.689 \pm 0.007, 0.305 \pm 0.023)	(0.686 \pm 0.016, 0.253 \pm 0.035)	(0.688 \pm 0.006, 0.256 \pm 0.023)	
BALD	(0.688 \pm 0.011, 0.313 \pm 0.012)	(0.686 \pm 0.015, 0.256 \pm 0.031)	(0.688 \pm 0.011, 0.263 \pm 0.011)	
ISAL	(0.697 \pm 0.002, 0.308 \pm 0.025)	(0.698 \pm 0.004, 0.274 \pm 0.022)	(0.697 \pm 0.001, 0.260 \pm 0.026)	
JTT-20	(0.646 \pm 0.009, 0.240 \pm 0.016)	(0.630 \pm 0.024, 0.141 \pm 0.028)	(0.646 \pm 0.009, 0.200 \pm 0.007)	
FIS	(0.690 \pm 0.002, 0.299 \pm 0.029)	(0.694 \pm 0.002, 0.241 \pm 0.035)	(0.698 \pm 0.005, 0.252 \pm 0.030)	

respectively. That is, the default validation set sizes are 1996 (CelebA), 1800 (Adult), and 247 (Compas) instances, respectively. In particular, given the smaller size of the default validation set, the minimum scale of the validation set size is set to $1/5 \times$ (nearly 400 CelebA images). Table 6 and Table 7 present the performance results on the CelebA, Adult, and Compas datasets, respectively.

E.5 Benchmarking Model Performance with Validation Set Enhancements

Note that we resort to an additional validation set for developing FIS. To demonstrate FIS's advantage at the same levels of information, we introduce a new baseline called Random+Val. This method involves continuing to train the model with a randomly sampled validation set. Specifically, we start with the Random's last saved checkpoint and train it further using the validation set. In particular, we would incorporate a fairness regularizer with dynamic weight to

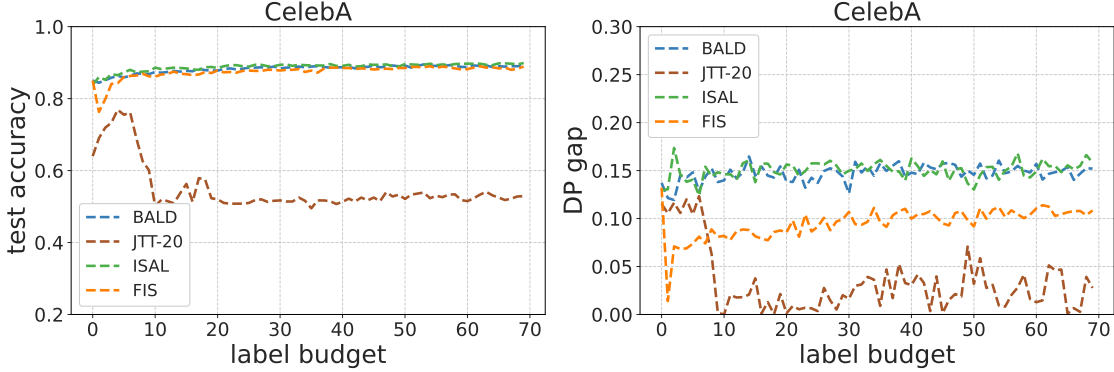


Figure 4: The impact of label budgets on the test accuracy & DP gap in the CelebA dataset. The binary classification targets is Smiling.

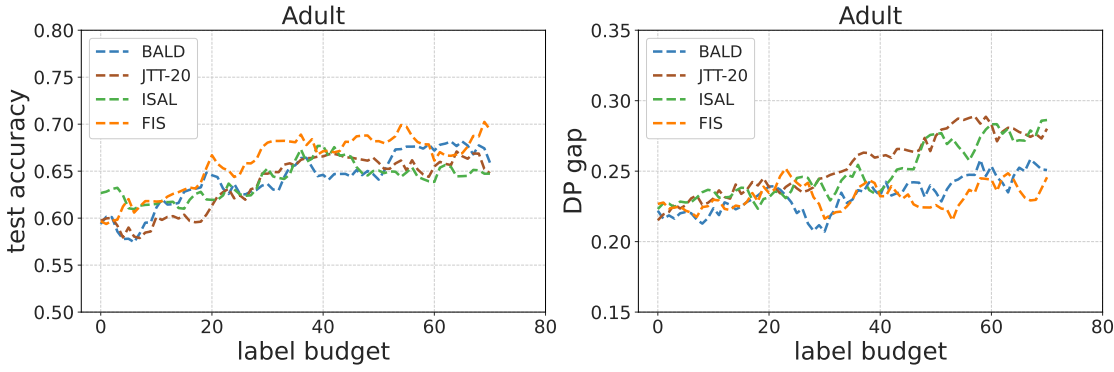


Figure 5: The impact of label budgets on the test accuracy & DP gap in the Adult dataset. The sensitive attribute is `sex`.

Table 6: The performance results of (test_accuracy, fairnessViolation) on the **CelebA dataset** when the validation set size is reduced to $1/2 \times$ and $1/5 \times$. Our algorithm retains the test accuracy and fairness violation when we vary the validation set size.

$\epsilon = 0.05$	Smiling			Attractive		
	DP	EOP	EOd	DP	EOP	EOd
$1 \times$	(0.848, 0.084)	(0.876, 0.031)	(0.864, 0.030)	(0.680, 0.285)	(0.695, 0.148)	(0.692, 0.148)
$1/2 \times$	(0.872, 0.105)	(0.891, 0.042)	(0.880, 0.028)	(0.648, 0.249)	(0.688, 0.188)	(0.678, 0.147)
$1/5 \times$	(0.872, 0.117)	(0.863, 0.057)	(0.886, 0.028)	(0.604, 0.171)	(0.707, 0.209)	(0.645, 0.145)

$\epsilon = 0.05$	Young			Big_Nose		
	DP	EOP	EOd	DP	EOP	EOd
$1 \times$	(0.766, 0.139)	(0.775, 0.043)	(0.769, 0.168)	(0.771, 0.156)	(0.765, 0.129)	(0.758, 0.155)
$1/2 \times$	(0.735, 0.093)	(0.762, 0.067)	(0.769, 0.055)	(0.771, 0.054)	(0.761, 0.162)	(0.748, 0.096)
$1/5 \times$	(0.743, 0.107)	(0.780, 0.097)	(0.757, 0.166)	(0.772, 0.095)	(0.750, 0.300)	(0.760, 0.156)

train the model using validation data, considering its sensitive attributes to reduce fairness disparity. Due to its small size, we limit training to 10 epochs to avoid overfitting. The performance results of Random, Random+Val, and FIS are given in Table 8.

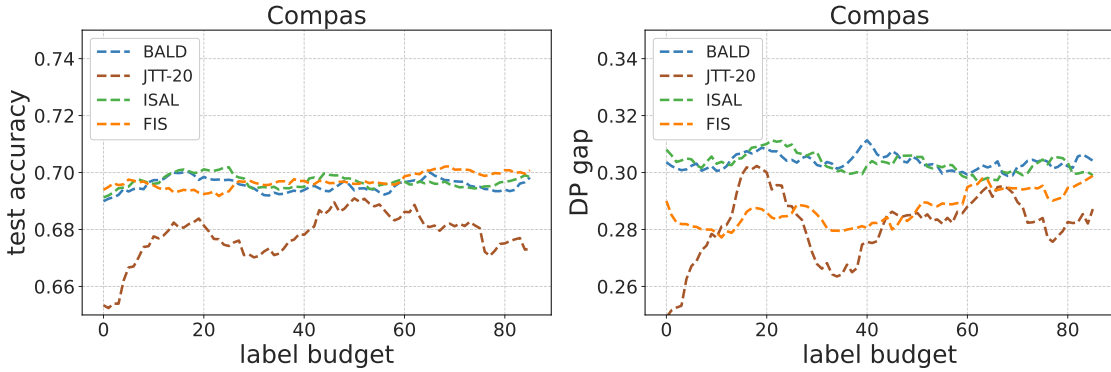


Figure 6: The impact of label budgets on the test accuracy & DP gap in the Compas dataset. The sensitive attribute is `race`.

Table 7: We examine the performance results of (`test_accuracy`, `fairnessViolation`) on the tabular datasets (**Left**: Adult; **Right**: Compas) when the validation set size is reduced to $1/2 \times$, $1/4 \times$, and $1/20 \times$. We observe that our algorithm still retains the test accuracy and fairness violation when we vary the validation set size.

$\epsilon = 0.05$	Adult - Income(Age)			Compas - Recidivism		
	DP	EOP	EOD	DP	EOP	EOD
$1 \times$	(0.757, 0.198)	(0.718, 0.124)	(0.750, 0.125)	(0.690, 0.313)	(0.696, 0.249)	(0.702, 0.257)
$1/2 \times$	(0.717, 0.259)	(0.634, 0.123)	(0.736, 0.143)	(0.683, 0.270)	(0.680, 0.247)	(0.693, 0.244)
$1/4 \times$	(0.749, 0.196)	(0.750, 0.121)	(0.747, 0.137)	(0.677, 0.283)	(0.682, 0.276)	(0.680, 0.244)
$1/20 \times$	(0.721, 0.205)	(0.706, 0.148)	(0.706, 0.179)	(0.689, 0.289)	(0.668, 0.236)	(0.683, 0.252)

Table 8: Comparative analysis of (`test_accuracy`, `fairnessViolation`) in the CelebA, Adult and Compas datasets. The table illustrates that even at the same information level (using the validation set to train), FIS can obtain better performances. Similarly, we highlight all the fairer but without sacrificing accuracy results in boldface compared to Random.

$\epsilon = 0.05$	CelebA - Smiling			CelebA - Attractive		
	DP	EOP	EOD	DP	EOP	EOD
Random	(0.853, 0.132)	(0.863, 0.053)	(0.861, 0.031)	(0.696, 0.367)	(0.708, 0.253)	(0.696, 0.243)
Random + Val	(0.801, 0.115)	(0.872, 0.139)	(0.879, 0.153)	(0.638, 0.199)	(0.699, 0.366)	(0.699, 0.355)
FIS	(0.877, 0.122)	(0.886, 0.040)	(0.882, 0.023)	(0.680, 0.285)	(0.695, 0.148)	(0.692, 0.148)

$\epsilon = 0.05$	Adult - Income(Age)			Compas - Recidivism		
	DP	EOP	EOD	DP	EOP	EOD
Random	(0.745, 0.236)	(0.729, 0.136)	(0.748, 0.151)	(0.696, 0.316)	(0.698, 0.258)	(0.694, 0.269)
Random + Val	(0.762, 0.161)	(0.743, 0.266)	(0.788, 0.131)	(0.604, 0.136)	(0.623, 0.147)	(0.628, 0.153)
FIS	(0.751, 0.205)	(0.725, 0.130)	(0.750, 0.125)	(0.688, 0.316)	(0.695, 0.250)	(0.693, 0.254)